J|A|C|S
ARTICLES
Published on Web 04/05/2007

β-Hydrogen Kinetic Effect

Raffaello Romeo,*,† Giuseppina D'Amico,† Emilia Sicilia,‡ Nino Russo,‡ and Silvia Rizzato§

Contribution from the Dipartimento di Chimica Inorganica, Chimica Analitica e Chimica Fisica, Università di Messina, Salita Sperone, 31-Vill. S. Agata-98166 Messina, Italy, Dipartimento di Chimica, Università della Calabria, I-87030 Arcavacata di Rende (Cs) Italy, and Dipartimento di Chimica Strutturale (DCSS) and Facoltà di Farmacia, Università di Milano, via Venezian 21, Milano, Italy

Received January 11, 2007; E-mail: rromeo@unime.it

Abstract: A combined kinetic and DFT study of the uncatalyzed isomerization of cationic solvent complexes of the type *cis*-$[Pt(R')(S)(PR_3)_2]^+$ (R′ = linear and branched alkyls or aryls and S = solvents) to their trans isomers has shown that the reaction goes through the rate-determining dissociative loss of the weakly bonded molecule of the solvent and the interconversion of two geometrically distinct T-shaped 14-electron three-coordinate intermediates. The Pt−S dissociation energy is strongly dependent on the coordinating properties of S and independent of the nature of R′. The energy barrier for the fluxional motion of $[Pt(R')(PR_3)_2]^+$ is comparatively much lower (≈8−21 kJ mol^{-1}). The presence of β-hydrogens on the alkyl chain (R′ = Et, Pr^n, and Bu^n) produces a great acceleration of the reaction rate. This accelerating effect has been defined as the β-hydrogen kinetic effect, and it is a consequence of the stabilization of the transition state and of the cis-like three-coordinate $[Pt(R')(PR_3)_2]^+$ intermediate through an incipient agostic interaction. The DFT optimization of $[Pt(R')(PMe_3)_2]^+$ (R′ = Et, Pr^n, and Bu^n) reproduces a classical dihapto Pt···η^2-HC agostic mode between the unsaturated metal and a dangling C−H bond. The value of the agostic stabilization energy (in the range of ≈21−33 kJ mol^{-1}) was estimated by both kinetic and computational data and resulted in being independent of the length of the hydrocarbon chain of the organic moiety. A better understanding of such interactions in elusive reaction intermediates is of primary importance in the control of reaction pathways, especially for alkane activation by metal complexes.

Introduction

Four-coordinated square-planar 16-electron transition metal compounds show a great steric and electronic propensity to add a fifth ligand and to form five-coordinate 18-electron species either as discrete compounds[1] or as reaction intermediates.[2] Yet, there is a great interest in the possibility of activating alternative low-energy dissociative pathways.[3] Many organometallic reactions are thought to take place through intermediates with open coordination sites, and dissociation, usually of a neutral ligand, is often proposed as the initial step in many reactions involving square-planar d^8 organometallic complexes.[4] This dissociation enables subsequent processes or initiates catalytic cycles. In platinum(II) chemistry, T-shaped three-coordinate 14-electron intermediates were assumed as key intermediates in reactions of β-hydrogen elimination,[5] thermal decomposition of dialkyls,[6] *trans*-[7] and *cis*-[8] monoalkyl compounds, insertion of olefins into the M−H bond,[9] electrophilic attack at the Pt−C bond,[10]

† Università di Messina.
‡ Università della Calabria.
§ Università di Milano.

(1) (a) Albano, V. G.; Natile, G.; Panunzi, A. *Coord. Chem. Rev.* **1994**, *133*, 67−114. (b) Maresca, L.; Natile, G. *Comments Inorg. Chem.* **1993**, *14*, 349−366.
(2) (a) Tobe, M. L.; Burgess, J. *Inorganic Reaction Mechanisms*; Addison-Wesley Longman: Essex, UK, 1999. (b) Wilkins, R. G. *Kinetics and Mechanisms of Reactions of Transition Metal Complexes*; VCH: Weinheim, Germany, 1991. (c) Atwood, J. D. *Inorganic Organometallic Reaction Mechanisms*; Brook/Cole: Monterey, CA, 1985. (d) Cross, R. *Ligand Substitution Reactions of Square-Planar Molecules*; The Royal Society of Chemistry: London, 1985. (e) Basolo, F.; Pearson, R. G. *Mechanisms of Inorganic Reactions*; Wiley: New York, 1968. (f) Langford, C. H.; Gray, H. B. *Ligand Substitution Processes*; W. A. Benjamin: New York, 1965.
(3) For a discussion on dissociative pathways in platinum(II) chemistry, see Romeo, R. *Comments Inorg. Chem.* **1990**, *11*, 21−57.
(4) (a) Collman, J. P.; Hegedus, L. S.; Norton, J. R.; Finke, R. C. *Principles and Applications of Organotransition Metal Chemistry*; University Science Books: Mill Valley, CA, 1987. (b) Crabtree, R. H. *The Organometallic Chemistry of the Transition Metals*; Wiley-Interscience: New York, 1994. (c) Yamamoto, A. *Organotransition Metal Chemistry*; Wiley: New York, 1986. (d) James, B. R. In *Comprehensive Organometallic Chemistry*; Wilkinson, G., Stone, F. G. A., Abel, E. W., Eds.; Pergamon Press: Oxford, 1982; Ch. 51. (e) Parshall, G. W. *Homogeneous Catalysis*; Wiley-Interscience: New York, 1980.
(5) For general reviews of β-elimination reactions, see: (a) Cross, R. J. *The Chemistry of the Metal−Carbon Bond*; Hartley, F. R., Patai, S., Eds.; John Wiley: New York, 1985; Vol. 2, Ch. 8. (b) Whitesides, G. M. *Pure Appl. Chem.* **1981**, *53*, 287−292. (c) Yamamoto, A.; Yamamoto, T.; Komiya, S.; Ozawa, F. *Pure Appl. Chem.* **1984**, *56*, 1621−1634.
(6) (a) McCarthy, T. J.; Nuzzo, R. G.; Whitesides, G. M. *J. Am. Chem. Soc.* **1981**, *103*, 3396−3403. (b) Griffiths, D. C.; Young, G. B. *Organometallics* **1989**, *8*, 875−886.
(7) (a) Brainard, R. L.; Whitesides, G. M. *Organometallics* **1985**, *4*, 1550−1557. (b) Brainard, R. L.; Miller, T. M.; Whitesides, G. M. *Organometallics* **1986**, *5*, 1481−1490.
(8) Alibrandi, G.; Cusumano, M.; Minniti, D.; Monsù Scolaro, L.; Romeo, R. *Inorg. Chem.* **1989**, *28*, 342−347.
(9) (a) Romeo, R.; Alibrandi, G.; Monsù Scolaro, L. *Inorg. Chem.* **1993**, *32*, 4688−4694. (b) Coussens, B. B.; Buda, F.; Oevering, H.; Meier, R. J. *Organometallics* **1998**, *17*, 795−801 and references therein. (c) Thorn, D. L.; Hoffmann, R. *J. Am. Chem. Soc.* **1978**, *100*, 2079−2090.
(10) (a) Romeo, R.; D'Amico, G. *Organometallics* **2006**, *25*, 3435−3446. (b) Romeo, R.; Minniti, D.; Lanza, S.; Uguagliati, P.; Belluco, U. *Inorg. Chem.* **1978**, *17*, 2813−2818.

10.1021/ja0702162 CCC: $37.00

geometrical isomerization,[11] exchange reactions,[12] and fluxional motions of coordinated ligands.[13] Another promising feature of unsaturated platinum(II) chemistry is ligand cycloplatination[14,15] or successful C−H activation under mild conditions by complexes of the form $[Pt(N-N)(CH_3)(solv)]^+$, where N−N is a bidentate nitrogen-centered ligand and solv is a weakly coordinating solvent.[16] Likewise, dissociative pathways were proposed for a number of cases in palladium(II) chemistry, isomerization, ligand rotation, β-elimination, and palladium-catalyzed cross-coupling reactions.[17]

Despite the kinetic perception of the intermediacy of such elusive coordinatively unsaturated intermediates in a number of fundamental organometallic processes, and their recognized importance in homogeneous catalysis and bond activation, direct proof of 14-electron platinum(II) complexes has been difficult to find. The reason is that unsaturation on the metal can be easily relieved by coordination of the solvent or of anions on forming 16-electron species, and dimerization is also a reasonable alternative. Very few papers have been published so far that describe the structural characterization of such compounds. Spencer et al. have described the cationic $[Pt(R)(P-P)]^+$ complexes (P−P = chelating ligand and R = ethyl, norbornyl) that show β-agostic C−H interactions (complex A in Chart 1),[18] Ingleson et al. have reported on the complex $[Pt(CH_3)(^iPr_3P)_2]^+$ that is stabilized by β-agostic C−H interactions (complex B in Chart 1),[19] and Baratta et al. have prepared Pt(II) cationic complexes *trans*-$[Pt(CH_3)L_2]^+$ supported by a δ-agostic interaction from the bulky phosphine PR_2-(2,6-$Me_2C_6H_3$), [R = Ph or Cy] (complex C in Chart 1).[20]

Chart 1. View of Some Cationic T-Shaped Platinum(II) Molecules Stabilized by Agostic Interactions

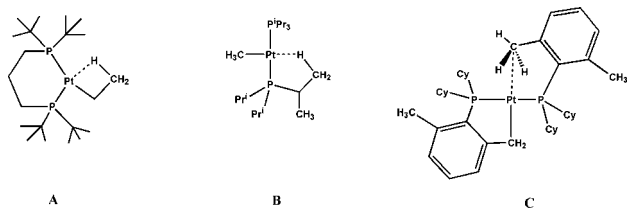

Related complexes of isoelectronic Ni(II),[21] Rh(I),[22,23] and Pd(II)[24−27] have also been described. Judging from the bonding and structural features of the species mentioned previously, the challenge to isolate stable 14-electron T-shaped compounds relies on the use of non-innocent, preferably bulky, ligands that guarantee some form of protection of the fourth coordination site and a certain extent of electron transfer through C−H···· M agostic interactions to a vacant orbital of the metal. Agostic interactions appear in a number of highly diverse transition and lanthanide metal compounds and have been scrutinized intensively by X-ray crystallography, NMR, or computational techniques.[28] The C−H····M interaction seems to be particularly favored by steric constraints brought about by bulky ligands.[29] Much less understood is the role of agostic interactions on the reactivity, although it appears to be crucial in the reaction of β-hydride elimination[5] as well as in the control of the tacticity of polymers.[30]

When an incipient β-agostic interaction by a dangling C−H bond stabilizes a T-shaped transient three-coordinate transition state or intermediate, this results in a sharp increase of the reaction rate. We discovered this phenomenon in kinetic studies of dissociative processes in platinum(II) chemistry, as ligand exchange and substitution performed on the novel complex *cis*-$[Pt(Hbph)_2(dmso)_2]$ ($Hbph^- = \eta^1$-biphenyl monoanion).[15,31] The

(11) (a) Romeo, R. *Comments Inorg. Chem.* **2002**, *23*, 79−100 and references therein. (b) Anderson, G. K.; Cross, R. J. *Chem. Soc. Rev.* **1980**, *9*, 185−215.
(12) Scott, J. D.; Puddephatt, R. J. *Organometallics* **1983**, *2*, 1643−1648.
(13) (a) Romeo, R.; Carnabuci, S.; Fenech, L.; Plutino, M. R.; Albinati, A. *Angew. Chem., Int. Ed.* **2006**, *45*, 4494−4498. (b) Romeo, R.; Carnabuci, S.; Plutino, M. R.; Romeo, A.; Rizzato, S.; Albinati, A. *Inorg. Chem.* **2005**, *44*, 1248−1262. (c) Romeo, R.; Fenech, L.; Carnabuci, S.; Plutino, M. R.; Romeo, A. *Inorg. Chem.* **2002**, *41*, 2839−2847. (d) Romeo, R.; Fenech, L.; Monsù Scolaro, L.; Albinati, A.; Macchioni, A.; Zuccaccia, C. *Inorg. Chem.* **2001**, *40*, 3293−3302.
(14) Romeo, R., Plutino, M. R., Romeo, A. *Helv. Chim. Acta* **2005**, *88*, 507−522.
(15) Plutino, M. R.; Monsù Scolaro, L.; Albinati, A.; Romeo, R. *J. Am. Chem. Soc.* **2004**, *126*, 6470−6484.
(16) (a) Williams, T. J.; Labinger, J. A.; Bercaw, J. E. *Organometallics* **2007**, *26*, 281−287. (b) Driver, T. G.; Williams, T. J.; Labinger, J. A.; Bercaw, J. E. *Organometallics*, **2007**, *26*, 294−301. (c) Lersch, M.; Tilset, M. *Chem. Rev.* **2005**, *105*, 2471−2526. (d) Labinger, J. A.; Bercaw, J. E. *Nature* **2002**, *417*, 507−514. (e) Zhong, H. A.; Labinger, J. A.; Bercaw, J. E. *J. Am. Chem. Soc.* **2002**, *124*, 1378−1399. (f) Johansson, L.; Tilset, M.; Labinger, J. A.; Bercaw, J. E. *J. Am. Chem. Soc.* **2000**, *122*, 10846−10855. (g) Procelewska, J.; Zahl, A.; van Eldik, R.; Zhong, H. A.; Labinger, J. A.; Bercaw, J. E. *Inorg. Chem.* **2002**, *41*, 2808−2810. (h) Johansson, L.; Ryan, O. B.; Tilset, M. *J. Am. Chem. Soc.* **1999**, *121*, 1974−1975. (i) Johansson, L.; Ryan, O. B.; Römming, C.; Tilset, M. *J. Am. Chem. Soc.* **2001**, *123*, 6579−6590. (j) Johansson, L.; Tilset, M. *J. Am. Chem. Soc.* **2001**, *123*, 739−740. (k) Holtcamp, M. W.; Henling, L. M.; Day, M. W.; Labinger, J. A.; Bercaw, J. E. *Inorg. Chim. Acta* **1998**, *270*, 467−478. (l) Periana, R. A.; Taube, D. J.; Gamble, S.; Taube, H.; Satoh, T.; Fujii, H. *Science* **1998**, *280*, 560−564. (m) Wick, D. D.; Goldberg, K. I. *J. Am. Chem. Soc.* **1997**, *119*, 10235−10236. (n) Fekl, U.; Goldberg, K. I. *Adv. Inorg. Chem.* **2003**, *54*, 259−320.
(17) (a) Minniti, D. *Inorg. Chem.* **1994**, *33*, 2631−2634. (b) Louie, J.; Hartwig, J. F. *J. Am. Chem. Soc.* **1995**, *117*, 11598−11599. (c) Casado, A. L.; Casares, J. A.; Espinet, P. *Inorg. Chem.* **1998**, *37*, 4154−4156. (d) Casares, J. A.; Coco, S.; Espinet, P.; Lin, Y. S. *Organometallics* **1995**, *14*, 3058−3067. (e) Gelling, A.; Orrell, K. G.; Osborne, A. G.; Sik, V. *J. Chem. Soc., Dalton Trans.* **1998**, 937−946. (f) Albéniz, A. C.; Casado, A. L.; Espinet, P. *Inorg. Chem.* **1999**, *38*, 2510−2515. (g) Albéniz, A. C.; Espinet, Martín-Ruiz, B. *Chem.—Eur. J.* **2001**, *7*, 2481−2489. (h) Brown, J. M.; Cooley, N. A. *Chem. Rev.* **1988**, *88*, 1031−1046. (i) Bartolomé, C.; Espinet, P.; Martín-Álvarez, J. M.; Villafaòe, F. *Eur. J. Inorg. Chem.* **2004**, 2326−2337. (j) Culkin, D. A.; Hartwig, J. F. *Acc. Chem. Res.* **2003**, *36*, 234−245. (k) Hartwig, J. F. *Pure Appl. Chem.* **1999**, *71*, 1417−1423. (l) Miyaura, N.; Yanagi, T.; Suzuki, A. *Synth. Commun.* **1981**, *11*, 513−519. (m) Milstein, D.; Stille, J. K. *J. Am. Chem. Soc.* **1979**, *101*, 4992−4998.
(18) (a) Carr, N.; Mole, L.; Orpen, A. G.; Spencer, J. L. *J. Chem. Soc., Dalton Trans.* **1992**, 2653−2662. (b) Mole, L.; Spencer, J. L.; Carr, N.; Orpen, A. G. *Organometallics* **1991**, *10*, 49−52.
(19) Ingleson, M. J.; Mahon, M. F.; Weller, A. S. *Chem. Commun.* **2004**, 2398−2399.
(20) Baratta, W.; Stoccoro, S.; Doppiu, A.; Herdtweck, E.; Zucca, A.; Rigo, P. *Angew. Chem., Int. Ed.* **2003**, *42*, 105−109.
(21) Hay-Motherwell, R.; Wilkinson, G.; Sweet, T. K. N.; Hursthouse, M. B. *Polyhedron* **1996**, *15*, 3163−3166.
(22) Yared, Y. W.; Miles, S. L.; Bau, R.; Reed, C. A. *J. Am. Chem. Soc.* **1977**, *99*, 7076−7078.
(23) Urtel, H.; Meier, C.; Eisenträger, F.; Rominger, F.; Joschek, J. P.; Hofmann, P. *Angew. Chem., Int. Ed.* **2001**, *40*, 781−784.
(24) Stambuli, J. P.; Bühl, M.; Hartwig, J. F. *J. Am. Chem. Soc.* **2002**, *124*, 9346−9347.
(25) Yamashita, M.; Hartwig, J. F. *J. Am. Chem. Soc.* **2004**, *126*, 5344−5345.
(26) Stambuli, J. P; Incarvito, C. D.; Bühl, M.; Hartwig, J. F. *J. Am. Chem. Soc.* **2004**, *126*, 1184−1194.
(27) Campora, J.; Gutiérrez-Puebla, E.; Lopez, J. A.; Monge, A.; Palma, P.; Del Rio, D.; Carmona, E. *Angew. Chem., Int. Ed.* **2001**, *40*, 3641−3644.
(28) (a) Brookhart, M.; Green, M. L. H. *J. Organomet. Chem.* **1983**, *250*, 395−408. (b) Brookhart, M.; Green, M. L. H.; Wong, L. *Prog. Inorg. Chem.* **1988**, *36*, 1−124. (c) Crabtree, R. H.; Hamilton, D. G. *Adv. Organomet. Chem.* **1988**, *28*, 299−338. (d) Clot, E.; Eisenstein, O. Structure and Bonding Book Series. In *Principles and Applications of Density Functional Theory in Inorganic Chemistry II*; Kaltsoyannis, N., McGrady, J. E., Eds.; Springer: Berlin, 2004; Vol. 113, pp 1−36. (e) Crabtree, R. H. *Angew. Chem., Int. Ed. Engl.* **1993**, *32*, 789−805. (f) Canty, A. J.; van Koten, G. *Acc. Chem. Res.* **1995**, *28*, 406−413. (g) Yao, W.; Eisenstein, O.; Crabtree, R. H. *Inorg. Chim. Acta* **1997**, *254*, 105−111. (h) Ogasawara, M.; Saburi, M. *Organometallics* **1994**, *13*, 1911−1917.
(29) (a) Cooper, A. C.; Clot, E.; Maseras, F.; Eisenstein, O.; Caulton, K. G. *J. Am. Chem. Soc.* **1999**, *121*, 97−106. (b) Ujaque, G.; Cooper, A. C.; Maseras, F.; Eisenstein, O.; Caulton, K. G. *J. Am. Chem. Soc.* **1998**, *120*, 361−365. (c) Jaffart, J.; Etienne, M.; Maseras, F.; McGrady, J. E.; Eisenstein, O. *J. Am. Chem. Soc.* **2001**, *123*, 6000−6013.
(30) (a) Grubbs, R. H.; Coates, G. W. *Acc. Chem. Res.* **1996**, *29*, 85−93. (b) Margl, P.; Deng, L.; Ziegler, T. *Organometallics* **1998**, *17*, 933−946. (c) Margl, P.; Deng, L.; Ziegler, T. *J. Am. Chem. Soc.* **1999**, *121*, 154−162.

Table 1. Selected ^1H and $^{31}P\{^1H\}$ NMR Data for *cis*- and *trans*-Monoalkyl/aryl Solvent Species Obtained upon Fast Protonolysis of *cis*-[Pt(R)(R′)(PEt_3)$_2$] (**1**−**9**) and Subsequent Isomerization[a]

		cis-[Pt(R)(CD_3CN)(PEt_3)$_2$]$^+$			*trans*-[Pt(R)(CD_3CN)(PEt_3)$_2$]$^+$	
	R	δ (^1H)	δ ($^{31}P_A$)[b]	δ ($^{31}P_B$)[c]	δ (^1H)	δ (^{31}P)
1	CH_3	0.27 (3H)	19.1 (1775)	11.8 (4170)	0.16 (3H)	22.8 (2687)
2	C_2H_5	1.62 (2H)	18.3 (1621)	13.2 (4345)	1.76 (2H)	22.0 (2871)
		0.70 (3H)			0.84 (3H)	
3	C_2D_5		18.6 (1609)	13.0 (4352)		22.5 (2848)
4	*n*-C_3H_7	0.95−0.72 (4H)	12.9 (1657)	18.3 (4312)	1.83−1.57 (4H)	21.9 (2857)
		0.45 (3H)			0.47 (3H)	
5	*n*-C_4H_9	1.85−0.85 (6H)	18.3 (1648)	13.0 (4331)	1.77−1.63 (6H)	21.7 (2861)
		0.53 (3H)			0.53 (3H)	
6	$CH_2Si(CH_3)_3$	0.25 (2H)	18.3 (1890)	10.3 (4226)	0.16 (2H)	18.9 (2721)
		−0.15 (9H)			−0.21 (9H)	
7	C_6H_5		15.0 (1690)	7.4 (4200)		20.1 (2680)
8	2-MeC_6H_4	2.25 (3H)	15.2 (1653)	5.7 (4228)	2.20 (3H)	19.1 (2694)
9	2,4,6-C_6H_2	2.24 (6H)	15.6 (1644)	2.8 (4249)	2.20 (3H)	17.8 (2713)
		1.95 (3H)			1.94 (6H)	

[a] Recorded in MeCN-d_3 as the solvent at 263 K for **2a**−**4a** and at 298 K for **1a**, **5a**−**8a**, and for all the trans derivatives (**1b**−**9b**). Chemical shifts (δ) are in ppm from TMS and H_3PO_4; coupling constants $^1J_{PtP}$ in Hz are given in parentheses. [b] P_A, phosphorus atom trans to the alkyl or to the aryl group.[c] P_B, phosphorus atom trans to the coordinated MeCN-d_3.

effect was found to be by far more significant in the uncatalyzed cis to trans isomerization of solvent *cis*-[Pt(R)(S)(PEt_3)$_2$]$^+$ (R = linear or branched alkyls and S = MeOH) complexes.[32]

This paper focuses on a phenomenon that so far has had only sporadic evidence and reports a combined kinetic and DFT study of the spontaneous isomerization of cationic *cis*-[Pt(R)(S)(PR_3)$_2$]$^+$ complexes (kinetic data in acetonitrile for PR_3 = PEt_3; S = CH_3CN; R = Me, Et, Et-d_5, Pr^n, Bu^n, CH_2SiMe_3, Ph, 2-MeC_6H_4, or 2,4,6-$Me_3C_6H_2$; computational data for PR_3 = PMe_3; R = Me or Et; S = CH_3CN, MeOH, DMSO, or benzene; R = Bu^n; S = CH_3CN or MeOH). Besides confirming a rare dissociative mode of activation, inferred from the kinetic analysis, the computational data allow for a measure of the energies and a better understanding of the bonding and structural features of the species intercepted along the potential energy surface (PES) of the reaction. In particular, the T-shaped 14-electron species, formed upon solvent dissociation from *cis*-[Pt(R)(S)(PMe_3)$_2$]$^+$, appear to be stabilized by interactions with the electron pair of a dangling C−H bond giving origin to what has been called the β-hydrogen kinetic effect. The structural and bonding characteristics of *cis*-[Pt(R)(PMe_3)$_2$]$^+$ have been analyzed in detail. The agostic stabilization energy was found to affect also the fluxional motion of the T-shaped cis 14-electron species toward its trans form. All this information is crucial in exploring the role of these fascinating elusive species in fundamental processes such as C−H bond activation.[16]

Results

Synthesis, Characterization, and Structure of the Complexes. The dialkyl and mixed alkyl-aryl *cis*-[Pt(R)(R′)(PEt_3)$_2$] complexes were synthesized by literature methods and characterized by ^1H and ^{31}P NMR. The dialkyls species **1**−**5** showed only one phosphorus resonance in the ^{31}P NMR spectra, and the alkyl-aryls **6**−**9** showed two resonances, with low values of $^1J_{PtP}$ coupling constants, typical of phosphorus atoms trans to carbon in platinum(II) complexes. A complete characterization and assignment of the resonances is reported in Supporting Information Table SI1. Addition of the stoichiometric amount of an ethereal solution of HBF_4 to a solution of the platinum complex in acetonitrile results in a selective cleavage of the Pt−C(alkyl) σ-bond, and in the formation of the cationic solvent complex *cis*-[Pt(R)(CH_3CN)(PEt_3)$_2$]$^+$ (**1a**−**9a**) and alkane liberation. Care must be taken to avoid a local excess of acid that leads to the protonolysis of the remaining R group.

The cis products can be recognized by ^1H and ^{31}P NMR, at room temperature for **1a** and **6a**−**9a** complexes, but a lower temperature (263 K) is required when R is an alkyl group containing β-hydrogens (compounds **2a**−**5a**). Satisfactory indications of the stereochemistry of **1a**−**9a** came from their ^{31}P NMR spectra that showed two ^{31}P resonances for two nonequivalent phosphane ligands, characterized by completely different values of a coupling constant with ^{195}Pt, as a consequence of the diverse trans influence of the alkyl/aryl or CH_3CN ligands ($^1J_{PtP} \approx 1700$ Hz for P_A, in a trans position to the carbon atom, and $^1J_{PtP} \approx 4200$ Hz for P_B trans to CH_3CN). There was no evidence for the build-up of any intermediate species upon electrophilic attack by the proton, even at low temperature. The subsequent isomerization reactions were monitored at appropriate times until the cis to trans conversion was complete. A collection of selected ^1H and ^{31}P NMR data for the monoalkyl and monoaryl cis and trans solvent isomers is reported in Table 1. A complete characterization and assignment of the resonances is given in the Experimental Procedures. Typical examples of ^{31}P NMR spectra of cationic *cis*- and *trans*-[Pt(Et)(CD_3CN)(PEt_3)$_2$]$^+$ solvent complexes are given in Supporting Information Figure SI2.

X-ray quality crystals of **5** were grown by diffusion of *n*-hexane into a dichloromethane solution of the complex. Details of the structure determination are given in the Experimental Procedures. Table 2 lists experimental and crystallographic data. Selected bond distances and angles are given in Table 3. An

(31) Dissociative substitution is rather common for complexes of the type *cis*-[Pt(C,C)(S,S)] (C is a strong σ-donor carbon group; S = thioether or sulfoxide), no matter whether the carbon atom comes from an alkyl, an aryl, or a metalated aryl ligand. See (a) Plutino, M. R.; Monsù Scolaro, L.; Romeo, R.; Grassi, A. *Inorg. Chem.* **2000**, *39*, 2712−2720. (b) Frey, U.; Helm, L.; Merbach, A. E.; Romeo, R. *J. Am. Chem. Soc.* **1989**, *111*, 8161−8165. (c) Alibrandi, G.; Minniti, D.; Monsù Scolaro, L.; Romeo, R. *Inorg. Chem.* **1989**, *28*, 1939−1943. (d) Alibrandi, G.; Bruno, G.; Lanza, S.; Minniti, D.; Romeo, R.; Tobe, M. L. *Inorg. Chem.* **1987**, *26*, 185−190. (e) Minniti, D.; Alibrandi, G.; Tobe, M. L.; Romeo, R. *Inorg. Chem.* **1987**, *26*, 3956−3958. (f) Lanza, S.; Minniti, D.; Moore, P.; Sachinidis, J.; Romeo, R.; Tobe, M. L. *Inorg. Chem.* **1984**, *23*, 4428−4833. (g) Lanza, S.; Minniti, D.; Romeo, R.; Moore, P.; Sachinidis, J.; Tobe, M. L. *J. Chem. Soc., Chem. Commun.* **1984**, 542−543. (h) Minniti, D. *J. Chem. Soc., Dalton Trans.* **1993**, 1343−1345.

(32) (a) Romeo, R.; Plutino, M. R.; Elding, L. I. *Inorg. Chem.* **1997**, *36*, 5909−5916.

Table 2. Experimental Data for the X-ray Diffraction Study of **5**

formula	$C_{20}H_{48}P_2Pt$
mol wt	545.61
T (K)	120 (2)
diffractometer	Brucker SMART CCD
cryst syst	triclinic
space group (no.)	$P\bar{1}$ (2)
a (Å)	8.9295(9)
b (Å)	10.267(1)
c (Å)	14.388(1)
α (deg)	99.620(2)
β (deg)	107.679(2)
γ (deg)	98.996(2)
V (Å^3)	1208.5(2)
Z	2
ρ_{calcd} (g cm^{-3})	1.499
μ (mm^{-1})	5.94
radiation	Mo Kα ($\lambda = 0.71073$ Å)
θ range (deg)	$1.53 < \theta < 26.03$
no. of data collected	11022
no. of independent data	4751
no. of obsd reflns (n_o)	4588
$[\lvert F_o\rvert^2 > 2.0\sigma(\lvert F\rvert^2)]$	
no. of param. refined (n_v)	208
R_{int}	0.0196
R^a (obsd refln)	0.0148
$R^2{}_w{}^b$ (obsd refln)	0.0369
GOF^c	1.075

[a] $R = \Sigma(\lvert F_o - (1/k)F_c\rvert)/\Sigma\lvert F_o\rvert$. [b] $R^2_w = [\Sigma w(F_o^2 - (1/k)F_c^2)^2/\Sigma w\lvert F_o^2\rvert^2]$. [c] GOF $= [\Sigma w(F_o^2 - (1/k)F_c^2)^2/(n_o - n_v)]^{1/2}$.

Table 3. Bond Lengths (Å) and Angles (deg) for **5**

Pt−C(5)	2.108 (2)	C(5)−Pt−C(1)	83.24(9)
Pt−C(1)	2.114 (2)	C(5)−Pt−P(1)	167.75(6)
Pt−P(1)	2.3002 (6)	C(1)−Pt−P(1)	86.70(6)
Pt−P(2)	2.3065 (6)	C(5)−Pt−P(2)	91.02(6)
C(1)−Pt−P(2)	172.52 (6)	Pt−C(1)−C(2)	111.82 (6)
P(1)−Pt−P(2)	99.55 (2)	Pt−C(5)−C(6)	112.42 (6)

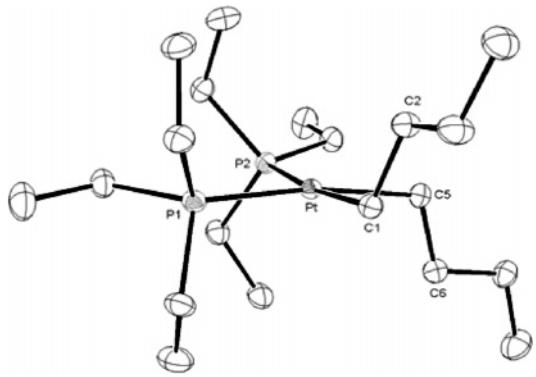

Figure 1. ORTEP view of a molecule of compound **5** showing 50% probability ellipsoids.

ORTEP view of the molecule is given in Figure 1. The immediate coordination sphere around the Pt center consists of the two alkyl groups, cis to each other, and the P atoms of the phosphane moieties. The square-planar coordination is tetrahedrically distorted with maximum deviation from the mean square plane (defined by atoms C(1), C(5), P(1), P(2), and Pt) of 0.118(1) Å. The butyl groups lie on opposite sides of the coordination plane with a slightly different orientation, as can be judged from the values of the C(1)−Pt−C(5)−C(6) and C(5)−Pt−C(1)−C(2) dihedral angles: 99.7(2) and 83.3(2)°, respectively. No significant difference is found in the Pt−C bond lengths (2.108(2) and 2.114(2) Å, respectively) or in the Pt−P bond lengths (2.3002 (6) and 2.3065 (6) Å, respectively). The Pt−P separations are in the upper range of the values found for other phosphane-dialkyl complexes of platinum(II).[33,34]

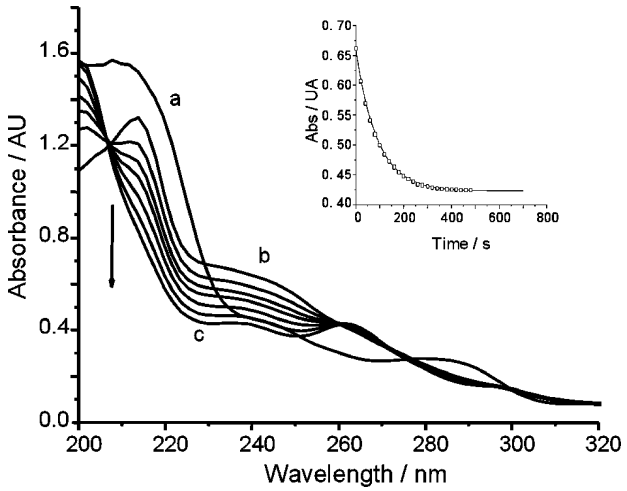

Figure 2. Electronic spectrum of **5** in CH_3CN at 298 K (a) and typical spectral changes (b → c) associated with the cis to trans isomerization of **5a** generated by protonolysis in situ. Cycle time for isomerization was 20 s. The inset in the figure gives the time dependence of the absorbance at 230 nm.

Kinetics. The isomerization of *cis*-$[Pt(R)(CH_3CN)(PEt_3)_2]^+$ complexes can be monitored by NMR techniques through the decrease of the two associated ^{31}P signals and the parallel and matching increase in the signal of the corresponding trans complex, which appears as a singlet with platinum satellites ($^1J_{PtP} \approx 2800$ Hz). However, the systematic kinetics of isomerization were followed spectrophotometrically by repetitive scanning of the spectrum in the UV region. The conversion was 100% complete, and the spectral changes showed well-defined isosbestic points (Figure 2).

The isomerization follows a first-order rate law. For R = Et (**2a**), Et-d_5 (**3a**), Pr^n (**4a**), or Bu^n (**5a**), the temperature dependence was measured with the traditional CTK method. Specific rate constants, k_i (s^{-1}), measured at different temperatures are given as Supporting Information in Table SI2 and were analyzed by least-squares regression of linear Eyring plots. Values of k_i (s^{-1}), $\Delta H^‡$ (kJ mol^{-1}), $\Delta S^‡$ (J K^{-1} mol^{-1}), and $\Delta G^‡$ (kJ mol^{-1}) at 298 K, for the same reactions, are collected in Table 4. The much slower conversions of the complexes in which R = CH_2SiMe_3 (**6a**), Ph (**7a**), 2-MeC_6H_4 (**8a**), or 2,4,6-$Me_3C_6H_2$ (**9a**) were measured with the VTK method,[35−37] and the kinetic and activation data calculated as described in the Experimental Procedures are listed in Table 4. In Figure 3 is plotted a typical example of a sigmoidal temperature−absorbance profile used to calculate the activation parameters for a slow reaction (isomerization of *cis*-$[Pt(CH_2SiMe_3)(CH_3CN)(PEt_3)_2]^+$, **6a**) and to construct a temperature−rate (k_i vs T) profile reported as Supporting Information Figure SI1B.

(33) Haar, C. M.; Nolan, S. P.; Marshall, W. J.; Moloy, K. G.; Prock, A.; Giering, W. P. *Organometallics* **1999**, *18*, 474−479.
(34) *International Tables for X-ray Crystallography*, 2nd ed.; Wilson, A. J. C., Prince, E., Eds.; Kluwer Academic Publishers: Dordrecht, The Netherlands, 1999; Vol. C, Ch. 9.5.
(35) Romeo, R.; Alibrandi, G. *Inorg. Chem.* **1997**, *36*, 4822−4830.
(36) (a) Alibrandi, G. *J. Chem. Soc., Chem. Commun.* **1994**, 2709−2710. (b) Alibrandi, G. *Inorg. Chim. Acta* **1994**, *221*, 31−34. (c) Alibrandi, G.; Micali, N.; Trusso, S.; Villari, A. *J. Pharm. Sci.* **1996**, *85*, 1105−1108. (d) Alibrandi, G.; Coppolino, S.; Micali, N.; Villari, A. *J. Pharm. Sci.* **2001**, *90*, 270−274.
(37) Zhang, S.; Brown, T. L. *Inorg. Chim. Acta.* **1995**, *240*, 427.

Table 4. Effect of Varying the Nature of R on Rates and Activation Parameters of Spontaneous Isomerization of *cis*-$[Pt(R)(CH_3CN)(PEt_3)_2]^+$ in Acetonitrile Solution

n	R	$10^6\ k_i$[a]	$\Delta H^{\ddagger}$[b,c]	$\Delta S^{\ddagger}$[d,e]	$\Delta G^{\ddagger}$[f]
1a	CH_3	2.42	147.7[c]	139[e]	106.3
2a	C_2H_5	4900	100.5[b]	48.2[d]	86.1
3a	C_2D_5	2730	99.8[b]	41.2[d]	87.5
4a	n-C_3H_7	8310	109.3[b]	81.9[d]	84.9
5a	n-C_4H_9	14000	95.9[b]	40.9[d]	83.7
6a	$CH_2Si(CH_3)_3$	40.2	117.1[c]	63.5[e]	98.2
7a	C_6H_5	15.8	127.9[c]	92.4[e]	100.4
8a	2-MeC_6H_4	8.09	129.2[c]	91.0[e]	102.1
9a	2,4,6-$Me_3C_6H_2$	12.7	115.1[c]	47.4[e]	101.0

[a] First-order rate constants (s^{-1}) for isomerization at 298.2 K. [b] Enthalpies of activation (kJ mol^{-1}) from constant-temperature kinetics. [c] Enthalpies of activation (kJ mol^{-1}) from variable-temperature kinetics. [d] Entropies of activation (J K^{-1} mol^{-1}) from constant-temperature kinetics. [e] Entropies of activation (J K^{-1} mol^{-1}) from variable-temperature kinetics. [f] Free energy of activation (kJ mol^{-1}) at 298.2 K.

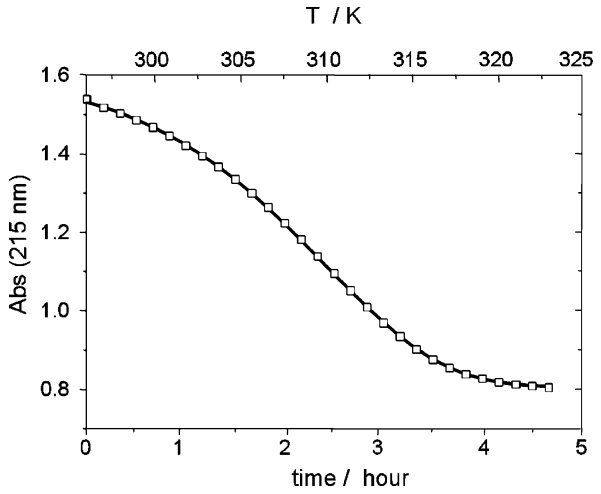

Figure 3. Change in optical density at 215 nm during the geometrical isomerization of *cis*-$[Pt(CH_2SiMe_3)(CH_3CN)(PEt_3)_2]^+$, **6a**, carried out in acetonitrile at the variable-temperature T (K) = 296 + 0.00156t (s).[38]

Computational Data. The analyzed processes, in the framework of DFT, were the geometrical conversion of the methyl and ethyl solvent complexes *cis*-$[Pt(R)(S)(PMe_3)_2]^+$ (R = Me or Et and S = acetonitrile, methanol, dimethyl-sulfoxide, or benzene) and of *cis*-$[Pt(Bu^n)(S)(PMe_3)_2]^+$ (S = acetonitrile or methanol). The aim was to obtain insight on the way in which the different nature of the alkyl group or of the labile coordinated solvent could affect the various steps along the reaction coordinate. Energy profiles for *cis*-$[Pt(Me)(CH_3CN)(PMe_3)_2]^+$ (Figure 4) and *cis*-$[Pt(Et)(CH_3CN)(PMe_3)_2]^+$ (Figure 5) show the key steps through which the cis to trans conversion proceeds.

The relevant computational data listed in Table 5 refer to the energetics of the isomerization of various species of *cis*-$[Pt(R)(S)(PMe_3)_2]^+$ in which the nature of the organic fragment (R = Me, Et, or Bu^n) and of the leaving group (CH_3CN, MeOH, Me_2SO, or benzene) has been systematically changed. Relative energies, calculated with respect to the reactant state, of the two T-shaped intermediates, of the transition state (TS) for their conversion, and of the product state are in kilojoules per mol.

Discussion

Kinetic Studies. We knew from previous studies[39] that bisphosphane solvent complexes of the type *cis*-$[Pt(R')(S)(PR_3)_2]^+$ (PR_3 = tertiary phosphine; R′= alkyl or aryl group; and S = solvent), formed easily in situ by protonolysis of precursor dialkyls or mixed alkyl-aryl platinum complexes, are short-lived species. The reason for their instability in solution is a facile conversion into long-standing trans isomers. The factors that usually combine in accelerating the rate of conversion are (i) electron release by the phosphine ligands,[35] (ii) steric repulsions and distortion of the original four-coordinate square-planar configuration,[35,11a] and (iii) interaction of the β-hydrogen atoms

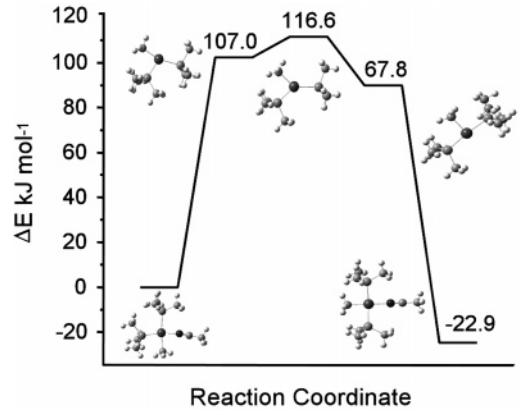

Figure 4. Calculated DFT PES for the isomerization of the solvent cationic complex $[Pt(Me)(MeCN)(PMe_3)_2]^+$.

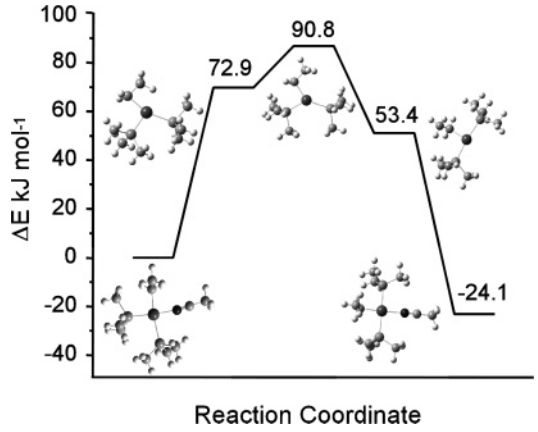

Figure 5. Calculated DFT PES for the isomerization of the solvent cationic complex $[Pt(Et)(MeCN)(PMe_3)_2]^+$.

Table 5. Effect of Varying Nature of R and Solvent on Relative Energies[a] of Optimized Structures of Two T-Shaped Reaction Intermediates, TS for Their Conversion, and Product during Isomerization of *cis*-$[Pt(R)(S)(PEt_3)_2]^+$[b] Complexes

n	R	S	cis T-shaped	TS	trans T-shaped	trans product
1	Me	CH_3CN	107.0	116.6	67.8	−22.9
2	Et	CH_3CN	72.9	90.8	53.4	−24.1
3	Bu^n	CH_3CN	66.9	85.6	52.6	−24.5
4	Me	MeOH	73.8	82.7	33.8	−15.1
5	Et	MeOH	32.5	50.5	13.0	−26.4
6	Bu^n	MeOH	25.9	48.9	11.7	−27.0
7	Me	Me_2SO	70.5	79.4	56.8	−10.5
8	Et	Me_2SO	35.1	53.1	15.6	−12.4
9	Me	C_6H_6	6.2	15.1	−7.6	−29.6
10	Et	C_6H_6	−27.0	−9.1	−46.5	−42.3

[a] Calculated with respect to the reactant (kJ mol^{-1}). [b] S = solvent.

(38) In a VTK experiment, the temperature increases linearly according to the general equation $T = T_0 + \gamma t$. In the kinetic run of Figure 3, T_0 = 296 K, and the temperature gradient is γ = 0.00156 K s^{-1}.

(39) (a) Alibrandi, G.; Minniti, D.; Monsù Scolaro, L.; Romeo, R. *Inorg. Chem.* **1988**, *27*, 318−324.

Scheme 1 Mechanism for Isomerization of Solvent Platinum(II) Cationic Complexes

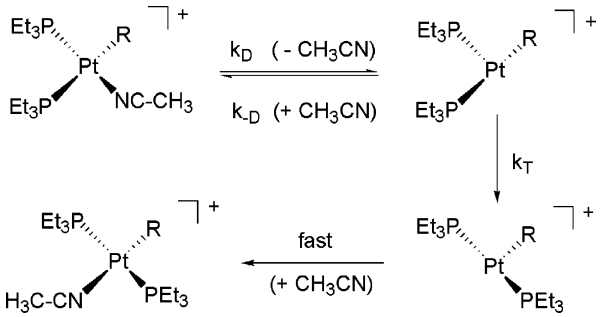

of the alkyl chain with the coordinatively unsaturated intermediate.[32,11a] The solvent plays a crucial role. In weakly coordinating solvents (benzene, dichloromethane, chloroform, etc.), the conversion is instantaneous. In protic solvents (methanol, ethanol, etc.), the process is relatively fast, and the characterization of the solvent cationic *cis*-$[Pt(R')(S)(PR_3)_2]^+$ complexes by NMR requires low-temperature measurements. In acetonitrile, a good coordinating solvent, the process can be conveniently followed by conventional or rapid-scanning spectrophotometry, and the characterization of cis solvent complexes is relatively easy as described previously. For all compounds, the conversion is complete, the spectral changes in the UV region show well-defined isosbestic points, the trans isomer is the only species at the end of the reaction, and the process follows a first-order rate law. The whole set of kinetic data is collected in Table 4, including the activation parameters that were calculated from the temperature dependence of the reaction using both the traditional isothermal (CTK) method and a non-isothermal (VTK) method. The advantages offered by the VTK method were discussed elsewhere[35,36] and are straightforward: (i) with a single kinetic run, it is possible to obtain a *k* versus *T* profile instead of a single rate constant, saving time and chemicals, (ii) the whole set of data comes from a single experiment carried out in homogeneous conditions, (iii) it permits fast and easy collection and processing of massive amounts of data, and (iv) the statistical error associated with the calculated values of $\Delta H^{\ddagger}$ and $\Delta S^{\ddagger}$ is very low. The large values of enthalpy of activation and particularly the positive entropies of activation associated with isomerization give an indication that the reaction proceeds through the well-established dissociative mechanism illustrated in Scheme 1, which involves dissociative loss of the solvent molecule and interconversion of two geometrically distinct three-coordinate T-shaped 14-electron intermediates.

A rate law of the form

$$k_i = k_D/\{1 + (k_{-D}/k_T)[S]\} \quad (1)$$

can be derived, in which the term $(k_{-D}/k_T)[S]$ measures the retardation due to the capture of the first intermediate by the bulk solvent. The mechanism is consistent with the great influence of the nature of the leaving group on the reaction rate. On going from *cis*-$[Pt(R)(MeOH)(PEt_3)_2]^+$ (rate data in ref 32) to *cis*-$[Pt(R)(CH_3CN)(PEt_3)_2]^+$ (rate data in Table 4), the rate of isomerization decreases by 3 orders of magnitude with a corresponding average increase of the free energy of activation of $\approx$15−20 kJ mol^{-1}. Electronic and steric features of cis groups having no β-hydrogens play a negligible role, if any, as can be judged from the comparison of the rate data in Table 4 for the compounds with R = Me, (trimethylsilyl)methyl, Ph, *o*-tolyl, or mesityl. The trend of the steric effects is significantly different from that observed for bimolecular nucleophilic substitutions[40] or for bimolecular electrophilic attack by H^+,[32] where the steric bulk of the cis group produces a decrease of 4−5 orders of magnitude in the rate.

β-Hydrogen Kinetic Effect. The rate of isomerization of *cis*-$[Pt(R)(CH_3CN)(PEt_3)_2]^+$ solvent complexes, when R = Et, Pr^n, or Bu^n, results in being many orders of magnitude higher than that of the remaining complexes. Inductive or steric effects cannot account for this large rate acceleration, and a specific interaction of β-hydrogens with the metal in the TS must be held responsible for the effect. A tentative calculation of the energy involved in the β-hydrogen kinetic effect, based on the values of the free activation energies listed in Table 4 and on the reasonable assumption that the ground state energies of **2a**, **4a**, and **5a** are comparable or not greatly different from that of **1a**, gives a mean value of 21.3 ± 1.3 kJ mol^{-1} for the stabilization energy of an agostic TS relative to that of a non-agostic TS (as the methyl compound **1a**). Interestingly, experimental and computational studies have revealed interaction energies for agostic bonds in transition metal complexes in the range of 40−50 kJ mol^{-1}.[41] The activation mode would be expected to exhibit a primary isotope effect when β-hydrogen atoms are replaced with deuterium atoms since bonds to the isotopic atoms are formed during that step.[42] There will be a preference for hydrogen over deuterium in the agostic interaction that would lead to a positive value of KIE (the kinetic isotope effect). Thus, the value of KIE (k_H/k_D = 1.8), obtained from the comparison of the rate data of **2a** and **3a** at 298.2 K, gives a further confirmation of an extensive involvement of hydrogen atoms in the formation of the transition state.

DFT Calculations: Mechanism, Structures, and Bonding. The PES's for isomerization obtained from DFT calculations for a variety of systems evolve along the same key steps indicated in Scheme 1, that is (i) ligand dissociation, (ii) conversion of a cis-like to a trans-like three-coordinate intermediate, and (iii) final uptake of the ligand by the latter. The relative energies, calculated with respect to the reactant state, of the two reaction intermediates, of the transition state for their rearrangement, and of the product state are collected in Table 5. The corresponding PES's, along with the structures of the stationary points, for the isomerization of *cis*-$[Pt(Me)(CH_3CN)(PMe_3)_2]^+$ and *cis*-$[Pt(Et)(CH_3CN)(PMe_3)_2]^+$ are illustrated in Figures 4 and 5, respectively. It appears that the most energy demanding step is ligand dissociation from the starting four-coordinate square-planar species, which can be assumed to be the rate-determining step. The most significant changes in the geometries of the original complexes that are observed along this reaction path are the crucial lengthening of the Pt−S bond

(40) Faraone, G.; Ricevuto, V.; Romeo, R.; Trozzi, M. *J. Chem. Soc., Dalton Trans.* **1974**, 1377−1380.
(41) (a) Gonzales, A. A.; Zhang, K.; Nolan, S. P.; Lopez de la Vega, R. L.; Mukerjee, S. L.; Hoff, C. D.; Kubas, G. J. *Organometallics* **1988**, *7*, 2429−2435. (b) Crabtree, R. H. *Chem. Rev.* **1985**, *85*, 245−269. (c) Zhang, K.; Gonzalez, A. A.; Mukerjee, S. L.; Chou, S.-J.; Hoff, C. D.; Kubat-Martin, K. A.; Barnhart, D.; Kubas, G. J. *J. Am. Chem. Soc.* **1991**, *113*, 9170−9176. (d) Lohrenz, J. C. W.; Woo, T. K.; Ziegler, T. *J. Am. Chem. Soc.* **1995**, *117*, 12793−12800. (e) Thomas, J. L. C.; Hall, M. B. *Organometallics* **1997**, *16*, 2318−2324. (f) Kawamura-Kuribayashi, H.; Koga, N.; Morokuma, K. *J. Am. Chem. Soc.* **1992**, *114*, 2359−2366.
(42) Melander, L.; Saunders, W. H. *Reaction Rates of Isotopic Molecules*; Robert E. Krieger: Malabar, FL, 1987; pp 170−201.

Chart 2. DFT Optimized Structures of T-shaped Three-Coordinate Intermediates for Geometrical Isomerization of *cis*-$[Pt(Et)(MeCN)(PMe_3)_2]^+$ and *cis*-$[Pt(Bu^n)(MeCN)(PMe_3)_2]^+$

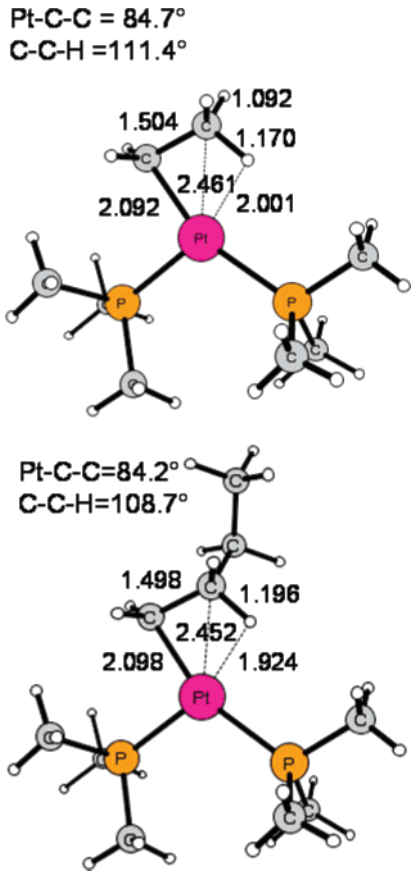

and a progressive narrowing of the M−C(1)−C(2) angle for the ethyl complex. The geometrically attractive trigonal-planar structure for the resulting three-coordinate $[Pt(R)(PMe_3)_2]^+$ species turns out to be less stable than a T-shaped configuration. In spite of the reduced symmetry, the surface maintains the same basic features shown by the more symmetric d^8 ML_3 class of compounds where a Jahn−Teller instability favors distortions to T- and Y-shaped configurations of lower energies.[43−45]

As can be seen from the structures displayed in Chart 2, the DFT optimization of the T-shaped intermediates *cis*-$[Pt(Et)(PMe_3)_2]^+$ and *cis*-$[Pt(Bu^n)(PMe_3)_2]^+$ reveals a classical dihapto Pt····η^2-HC agostic mode between the unsaturated metal and the dangling C−H bond of the same molecular fragment.[28] Focusing on *cis*-$[Pt(Et)(PMe_3)_2]^+$, the C(2)−H(3) bond lies in the Pt, C(1), C(2) plane (the dihedral angle Pt−C(1)−C(2)−H(3) = 0.916°), and the agostic bond is revealed by the considerable elongation of the bond length (1.170 Å) relative to the geminal non-agostic C(2)−H(4)(5) bond lengths (1.092 Å) that point away from the metal. The Pt−H(3) distance is 2.001 Å, and the close proximity of Pt and C−H is the result of the reduction of the Pt−C(1)−C(2) angle to 84.7°, as compared to 112.6° in the starting *cis*-$[Pt(Et)(CH_3CN)(PMe_3)_2]^+$ or 111.8° in the precursor dialkyl *cis*-$[Pt(Bu^n)_2(PEt_3)_2]$, and of a similar contraction of the C(1)−C(2)−H(3) angle to 111.4, while the other bond angles are slightly wider than the tetrahedral value. All these data fit well with the distinction made by Mealli et al.[46] between classical and nonclassical metal···H_3C−C interactions as a result of a close examination of the structural properties of a large amount of agostic compounds.

Therefore, the structural parameters of the reaction intermediates depicted in Chart 2 can be interpreted as arising from an agostic interaction viewed in a traditional way, which should involve electron donation from the σ C−H bond to the metal center and possible back-donation from suitable d orbitals of the metal to the σ^* C−H bond. Calculations carried out on *cis*-$[Pt(Me)(PMe_3)_2]^+$ accurately predict the T-shaped geometry and give reasonable values of the bond distances. According to the distortion process from trigonal planarity toward a T-shaped geometry, the molecular orbital calculations carried out by us reveal that the most external metal degenerate *xy* and $x^2 - y^2$ orbitals are split. As a result, the *xy* orbital is stabilized and together with the s orbital contributes to the formation of a linear s−d hybrid giving rise to a three-center—four-electron interaction with the alkyl and one of the phosphane ligands. The set of bonds in the coordination plane is completed with a bond with the remaining phosphorus atom that is characterized by a strong electrostatic component, while all the remaining d metal orbitals are doubly occupied. The situation is similar to that described by Landis et al.[47] in computing the shape of PdH_3^- and of other transition metal hydrides and alkyls by use of the (HV−VB) MM method. The drawing of the LUMOs of the non-agostic and agostic three-coordinate T-shaped species (Chart 3) highlights the disposability of a vacant σ^* Pt−P bond to accept electron donation from a weak Lewis base as the alkane C−H bond. This kind of interaction is prevented in *cis*-$[Pt(Me)(PMe_3)_2]^+$ but becomes feasible for alkyl groups containing β-hydrogens.

To obtain deeper insight into the nature of the interaction between the C−H bond and the valence orbitals of the metal atom, an NBO analysis[48] was carried out that identifies and estimates the magnitude of the interaction between each donor and each acceptor NBO. The main contribution is due to the electron density donation from the C−H σ-bond to the antibonding Pt−P σ^* NBO obtained by the out-of-phase overlap of the metal and phosphorus sd and sp^3 hybrids, respectively. It is also possible for the metal to back-donate into the empty orbitals of the ligand, and the same analysis calculates that the extent of this effect is greatest for the interaction between the Pt $d_{x^2-y^2}$ lone pair and the C−H σ^* NBO.

The energy stabilization associated with the agostic interaction, at a level of T-shaped reaction intermediates, has been estimated for *cis*-$[Pt(Et)(PMe_3)_2]^+$ by eliminating this interaction through a rotation of the ethyl group (60°) around the C_1-C_2 bond. The resulting structure with the ethyl group in the internally staggered conformation was therefore optimized, and the transition state for the rotation around the C(1)−C(2) bond

(43) For previous theoretical discussions of T geometries for low spin binary three-coordinate d^8 complexes, see: (a) Burdett, J. K. *J. Chem. Soc., Faraday Trans. 2* **1974**, *70*, 1599−1613. (b) Burdett, J. K. *Inorg. Chem.* **1975**, *14*, 375−382. (c) Elian, M.; Hoffmann, R. *Inorg. Chem.* **1975**, *14*, 1058−1076.
(44) Komiya, S.; Albright, T. A.; Hoffmann, R.; Kochi, J. K. *J. Am. Chem. Soc.* **1976**, *98*, 7255−7265.
(45) Tatsumi, K.; Hoffmann, R.; Yamamoto, A.; Stille, J. K. *Bull. Chem. Soc. Jpn.* **1981**, *54*, 1857−1867.
(46) Baratta, W. M; Mealli, C.; Herdtweck, E.; Ienco, A.; Mason, S. A.; Rigo, P. *J. Am. Chem. Soc.* **2004**, *126*, 5549−5562.
(47) Landis, C. R.; Cleveland, T.; Firman, T. K. *J. Am. Chem. Soc.* **1998**, *120*, 2641−2649.
(48) (a) Carpenter, J. E.; Weinhold, F. *J. Mol Struct.* **1988**, *169*, 41. (b) Carpenter, J. E.; Weinhold, F. J. *The Structure of Small Molecules and Ions*; Plenum: New York, 1988.

Chart 3. Drawings of (a) DFT Optimized Structure of *cis*-$[Pt(Me)(PMe_3)_2]^+$, (b) Its Computed LUMO, and (c) Computed LUMO of Corresponding Agostic *cis*-$[Pt(Et)(PMe_3)_2]^+$

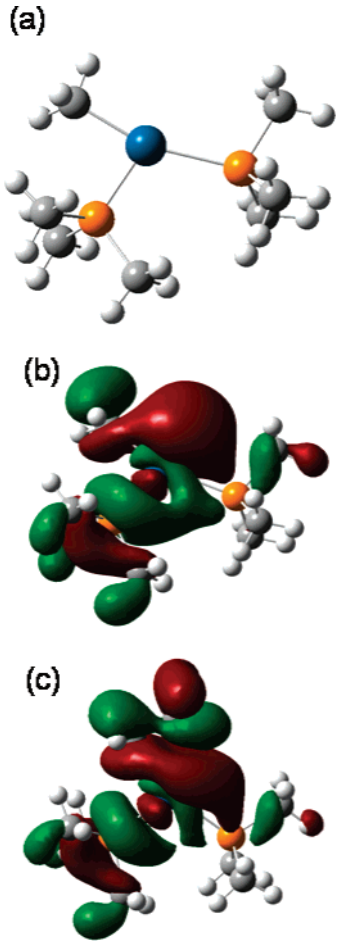

was located at 12.6 kJ mol^{-1} above the corresponding minimum. However, as noted recently for the case of $La(CH_2-SiH_3)_3$,[49] the rotation removes the agostic interaction but changes the conformation of the ligand from eclipsed in the agostic geometry to staggered in the transition state. The energy stabilization with respect to the structure with no β-agostic interaction, estimated including the energy for the conformational change (11.9 kJ mol^{-1} for CH_3-CH_3), was calculated as 24.5 kJ mol^{-1}, a value very near to that derived from the kinetic data for the TS. Values ranging from 30.9 to 59.4 kJ mol^{-1}, as a function of the used level of theory, were reported by Meier et. al for $[Pt(Et)(PH_3)_2]^+$, a product resulting from C_2H_4 insertion into the three-coordinate hydride $[Pt(H)(PH_3)_2]^+$.[9b] The rotation of the agostic bond away from the metal induces a widening of the $Pt-C_1-C_2$ angle from 84.7 to 97.6°, which testifies a residual degree of angular distortion, possibly due to the onset of electrostatic interactions. The energetic weakness of the agostic bond in the ethyl intermediate, despite the strong electrophilicity of the unsaturated metal, is not surprising since the C−H σ-bond is both strong and nonpolar, the HOMO σ is low-lying and therefore is ill-suited for electron donation, and the LUMO σ* is high in energy and unsuitable for accepting electron density. Hydrogen agostic interactions of this type, while lowering the energy of the formally three-coordinate 14-electron species, are insufficiently

(49) Perrin, L.; Maron, L.; Eisenstein, O.; Lappert, M. F. *New J. Chem.* **2003**, *27*, 121−127.

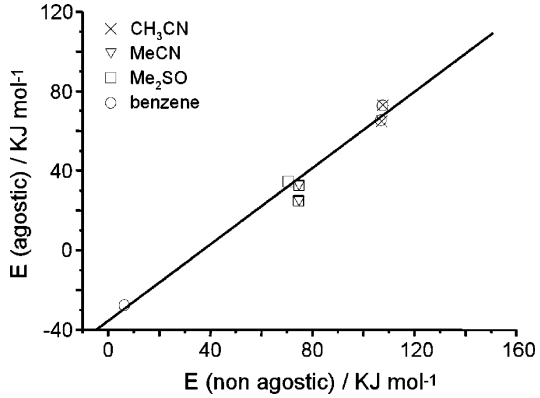

Figure 6. Correlation between the energies of agostic and non-agostic T-shaped intermediates.

stabilizing to allow such species to be isolated and characterized. Almost all the isolated three-coordinate complexes of d^8 transition metals mentioned in the Introduction contain an agostic interaction at the open site of a T-shaped geometry, but it must be borne in mind that the presence of bulky ligands plays a major role in helping to achieve the 16-electron configuration and in increasing the stability of the agostic bond.[29] However, the recent isolation and structural characterization of some aryl palladium amido complexes by Hartwigh et al.[25] has provided clear-cut evidence for the existence of true T-shaped three-coordinate 14-electron species with no donor in the open coordination site.

Leaving Group Effect. Previous detailed kinetic investigations on the spontaneous isomerization of *cis*-$[Pt(R)X(PR_3)_2]$ (R = alkyl or aryl groups and X = halide ions) complexes have indicated that the rate is extremely sensitive to structural changes influencing bond dissociation, viz. the nature of the halide ion, electrophilic solvation of the leaving halide ion through hydrogen bonding, and the amount of electronic density or strain at the metal atom, brought about by substituents on the aromatic ring, etc.[50] The present study has confirmed that Pt−S bond dissociation is the rate-determining step of the whole multistep process and that the lability of the coordinated solvents, judging from the energy involved in the formation of the cis-like T-shaped 14-electron three-coordinate intermediate (see data in Table 5), is $CH_3CN < MeOH \approx Me_2SO \ll$ benzene. This result is not surprising since it reflects perfectly the relative donor ability of the solvents.

A further consideration comes from the data listed in Table 5. On plotting the dissociation energies involved in the formation of the agostic intermediates *cis*-$[Pt(Et)(PMe_3)_2]^+$ and *cis*-$[Pt(Bu^n)(PMe_3)_2]^+$ against those for the formation of the non-agostic *cis*-$[Pt(Me)(PMe_3)_2]^+$, for various leaving groups (solvents), one obtains a linear plot with a value of the slope very near to the unit (Figure 6, slope = 0.960 ± 0.07, constant = −35.69 ± 5.9 kJ mol^{-1}, r^2 = 0.977). This linear relationship strongly suggests that the energy involved in the formation of the β-hydrogen interactions is hardly dependent on the nature

(50) (a) Faraone, G.; Ricevuto, V.; Romeo, R.; Trozzi, M. *J. Chem. Soc. A* **1971**, 1877−1881. (b) Romeo, R.; Minniti, D.; Trozzi, M. *Inorg. Chem.* **1976**, *15*, 1134−1138. (c) Romeo, R.; Minniti, D.; Lanza, S. *Inorg. Chem.* **1979**, *18*, 2362−2368. (d) Romeo, R. *Inorg. Chem.* **1978**, *17*, 2040−2041. (e) Romeo, R.; Minniti, D.; Lanza, S. *Inorg. Chem.* **1980**, *19*, 3663−3668. (f) Blandamer, M. J.; Burgess, J.; Romeo, R. *Inorg. Chim. Acta* **1982**, *65*, 179−180. (g) Blandamer, M. J.; Burgess, J.; Minniti, D.; Romeo, R. *Inorg. Chim. Acta* **1985**, *96*, 129−135. (h) Alibrandi, G.; Monsù Scolaro, L.; Romeo, R. *Inorg. Chem.* **1991**, *30*, 4007−4013.

of the group that is leaving the coordination sphere of the metal. Even the length of the alkyl chain plays a little, if any, role on the stability of the T-shaped species. These observations could help to elucidate the kinetic pathway for the {C−H } + M → {C−H···M} process. It would seem that the progress of the agostic interaction goes along with the departure of the leaving group (S) from the metal without affecting significantly the energy involved in the Pt−S bond breaking. The activation mode seems to feature that of a dissociative interchange (I_d, in the Langford−Gray terminology)[2f] nucleophilic substitution reaction, where the degree of assistance within a preformed aggregate (ion pair or reaction intermediate) is small and the reaction is primarily dissociative. The value of the constant of the plot, 35.69 ± 5.9 kJ mol^{-1}, represents the average difference between the energy of *cis*-[Pt(Me)(PMe_3)$_2$]$^+$ and that of the longer alkyl chain agostic T-shaped intermediates.

Fluxional Behavior of T-Shaped [Pt(R)(PMe_3)$_2$]$^+$ Species. The T-shaped configurations of the 14-electron species are energy minima along the PES for the geometrical isomerization of square-planar 16-electron species, and their interconversion occurs via a Y-shaped configuration. The basic features of the PES for such a conversion have been already obtained by Hoffmann et al. by extended Hückel calculations for the trialkylgold(III) complex $(CH_3)_3Au$[44] and for less symmetrical PdL_2R and $PdLR_2$ systems.[45] The structure and bonding features of *cis*-[Pt(R)(PMe_3)$_2$]$^+$ have been discussed in detail previously. As for its geometrical isomer, it makes use of a sd hybrid orbital[51] in the formation of coordination bonds with ligands but does not exhibit agostic interactions. The energy involved in the rearrangement of the cis-like to its trans-like T-shaped configuration is very small (average = 9.1 ± 0.4 kJ mol^{-1}) when the cis R group is CH_3 (data points 1, 4, 7, and 9 in Table 5), in agreement with the low-energy barrier indicated for the fluxionality of other coordinatively unsaturated unsymmetrical species such as [HPt(PH_3)$_2$]$^+$,[9c] [(Et)$_2$(PEt_3)Pt][6a], or [(Me)(PH_3)$_2$-Pd].[45] The energy barrier associated to the polytopal rearrangement when the R group contains β-hydrogens (Et or Bu^n) is doubled (average = 18.9 ± 2 kJ mol^{-1}). This would suggest that the conversion of an agostic cis-like three-coordinate to its trans form requires a supplementary consumption of energy and that this additional request of energy could result in an inhibition of the whole process if the constraint (electronic interactions or steric hindrance) in the three-coordinate species becomes compelling. In light of the experimental remarkable stability of species containing strong β-agostic C−H interactions, such as the cationic [Pt(Et)(P−P)]$^+$,[18] [Pt(CH_3)(^{i}Pr$_3$P)$_2$]$^+$,[19] or [Pd(Et)-(P−P)]$^+$[52] complexes and the substantial energy barrier calculated for geometrical conversion of [Pd(PH_3)(CH_3)$_2$],[45] it is easy to conclude that much more remains to be understood in the polytopal rearrangement of 14-electron T-shaped species.

Conclusion

The present article analyzes kinetic and computational aspects of the spontaneous cis−trans isomerization of cationic solvent alkyl/aryl platinum(II) complexes of the type *cis*-[Pt(R)(S)L$_2$]$^+$. Ligand (S) dissociation is the rate-determining step of the overall process, a rarity in platinum(II) chemistry, and the energy of the process is strongly dependent on the donor ability of S. The bonding features of the T-shaped 14-electron *cis*-[Pt(R)L$_2$]$^+$ species formed upon dissociation of a molecule of solvent were analyzed, with particular regard to the characteristics of the β-hydrogen interaction developed between the unsaturated metal ion and a dangling C−H bond of an alkyl group. The formation of hydrogen interactions in elusive reaction intermediates is a phenomenon strictly related to the coordination of a C−H bond to a transition metal, a problem of fundamental interest for catalytic reactions and for alkane functionalization via C−H bond activation. The β-agostic interaction in the T-shaped 14-electron *cis*-[Pt(R)L$_2$]$^+$ species developed in terms of a classical dihapto M···η^2-HC bonding, with a LUMO liable to electron donation by the hydrocarbon moiety and back-bonding from d orbitals to the C−H σ*-bonding orbital, with all Pt, C(1), C(2), and H atoms lying in a plane, a long C−H bond, a short M···H bond, and a pronounced narrowing of the Pt−C1−C2 angle. The stabilization of the intermediate and of the TS results in a sharp increase of the rate of isomerization. This phenomenon has been defined as the β-hydrogen kinetic effect to be distinguished from that usually investigated by spectroscopic techniques in stable transition metal and lanthanide complexes. The strength of the β-agostic interaction in the TS and intermediate has been estimated by both kinetic and DFT methods ranging from 20 to 33.5 kJ mol^{-1}, and it was found to not depend on the length of the hydrocarbon chain. The analysis of the computational data on the optimized structures of T-shaped 14-electron species *cis*-[Pt(R)(PMe_3)$_2$]$^+$ (R = Me, Et, or Bu^n), obtained from dissociation of different molecules of solvents (CH_3CN, MeOH, Me_2SO, or benzene) suggests that the formation of β-hydrogen interactions is entirely unaffected by the nature of the leaving group, and therefore, such forces play little if any role in the process of Pt−S bond breaking. The energy barrier associated to the fluxional rearrangement between T-shaped coordinatively unsaturated unsymmetrical [Pt-(R)L$_2$]$^+$ intermediates is very small (average = 9.1 ± 0.4 kJ mol^{-1}) when the cis R group is CH_3 but increases when the R group contains β-hydrogens (Et or Bu^n) (average = 18.9 ± 2 kJ mol^{-1}). An easy prediction is that as long as the strength of the agostic interactions increases, isomerization is prevented, and the possibility of isolation of reaction intermediates augments.

Experimental Procedures

General Procedures and Chemicals. All syntheses were performed on a double-manifold Schlenk vacuum line under a dry and oxygen-free dinitrogen atmosphere using freshly distilled, dried, and degassed solvents. Solvents employed in the synthetic procedures (Analytical Reagent Grade, Lab-Scan Ltd.) were distilled under nitrogen from sodium-benzophenone ketyl (tetrahydrofuran, diethyl ether, and toluene) or barium oxide (dichloromethane).[53] Phosphane ligands (from Strem) were used without any purification. Acetonitrile spectrophotometric grade for kinetic studies and CD_3CN for NMR measurements were used as received from Aldrich Chemical Co.

Instrumentation and Measurements. NMR analyses were performed on a Bruker AMX-R 300 spectrometer equipped with a broadband probe operating at 300.13 and 121.49 MHz for ^{1}H and ^{31}P nuclei, respectively. ^{1}H chemical shifts are reported in ppm (δ) with

(51) The distortion toward the T-shaped trans isomer stabilizes the $d_{x^2-y^2}$ orbital, the other component of the half-filled e′.

(52) Clegg, W.; Eastham, G. R.; Elsegood, M. R. J.; Heaton, B. T.; Iggo, J. A.; Tooze, R. P.; Whyman, R.; Zacchini, S. *Organometallics* **2002**, *21*, 1832−1840.

(53) Riddick, J. A.; Bunger, W. B.; Sakano, T. K. In *Organic Solvents*, 4th ed.; Weissberger, A., Ed.; Wiley & Sons: New York, 1986.

respect to Me_4Si and referenced to the residual protiated impurities of the deuterated solvent. Coupling constants are given in hertz. ^{31}P chemical shifts, in parts per million, are given relative to external phosphoric acid. The temperature within the probe was checked using the methanol method.[54] Slow reactions were carried out in a silica cell in the thermostated cell compartment of a JASCO V-560 or of a rapid-scanning Hewlett-Packard Model 8452 A spectrophotometer, with a temperature accuracy of 0.02 °C.

Synthesis of Complexes. The dialkyl substrates *cis*-$[Pt(R)_2(PEt_3)_2]$ (R = methyl (**1**),[55] ethyl (**2**),[56] ethyl-d_5 (**3**),[6a] *n*-propyl (**4**),[6a] *n*-butyl (**5**),[31c] or silyl (**6**)[57]) and the mixed alkyl-aryl complexes *cis*-[Pt(Me)(R)$(PEt_3)_2$] (R = phenyl (**7**),[39] *o*-tolyl (**8**),[32] or mesityl (**9**),[39]) are well-known compounds that were prepared by literature methods. The identity and purity of these compounds were established by elemental analysis and by ^1H and ^{31}P {^1H} NMR spectra. Elemental analyses were consistent with the theoretical formulas. A complete assignment of the ^1H and ^{31}P NMR resonances of these compounds is reported in Supporting Information Table SI1.

Monoalkyl/aryl Solvent Complexes. (a) *cis*-$[Pt(R)(CH_3CN\text{-}d_3)(PEt_3)_2]^+$ (1a−9a). For R = Et, Et-d_5, Pr^n, and Bu^n (**2a**−**5a**), the protonolysis was carried out at low temperature. A solution of an appropriate amount (5−6 mg, 0.01 mmol) of *cis*-$[Pt(R)_2(PEt_3)_2]$ in CD_3CN was frozen in the NMR tube before adding with a syringe HCF_3SO_3 in CD_3CN (in a 1:1 ratio, with respect to the complex). The temperature was slowly increased to 263 K, and the ^1H and ^{31}P NMR spectra of the ensuing *cis*-monoalkylsolvent species were recorded. For all the other compounds, (**1a** and **6a**−**9a**), the acid attack was carried out very carefully at 298 K, avoiding a local excess of acid concentration.

***cis*-$[Pt(Me)(CH_3CN\text{-}d_3)(PEt_3)_2]^+$ (1a).** ^1H NMR (CD_3CN, $T = 298$ K): δ 1.71 (m, $^3J_{HH} = 7.7$ Hz, 6H, P_A-*CH*$_2$-CH_3), 1.66 (m, $^3J_{HH} = 7.7$ Hz, 6H, P_B-*CH*$_2$-CH_3), 0.90 (m, $^3J_{HH} = 7.7$ Hz, 9H, P_A-CH_2-*CH*$_3$), 0.85 (m, $^3J_{HH} = 7.7$ Hz, 9H, P_B-CH_2-*CH*$_3$), 0.27 (m, $^2J_{PtH} = 51.7$ Hz, $^3J_{PH} = 6.6$ Hz, 3H, Pt-*CH*$_3$). $^{31}P\{^1H\}$ NMR (CD_3CN, $T = 298$ K): δ 19.1 (d, $^1J_{PtPA} = 1775$ Hz, $^2J_{PAPB} = 16.5$ Hz, P_A trans to CH_3), 11.8 (d, $^1J_{PtPB} = 4170$ Hz, $^2J_{PAPB} = 16.5$ Hz, P_B trans to MeCN).

***cis*-$[Pt(Et)(CH_3CN\text{-}d_3)(PEt_3)_2]^+$ (2a).** ^1H NMR (CD_3CN, $T = 263$ K): δ 1.62 (m, $^3J_{HH} = 7.7$ Hz, 2H, Pt-C*H*$_2$-CH_3), 1.38 (m, $^3J_{HH} = 7.8$ Hz, 12H, P_A-*CH*$_2$ + P_B-*CH*$_2$), 0.70 (m, $^3J_{HH} = 7.7$ Hz, 3H, Pt-CH_2-*CH*$_3$), 0.61 (m, $^3J_{HH} = 7.7$ Hz, 18H, P_A-*CH*$_3$ + P_B-*CH*$_3$). $^{31}P\{^1H\}$ NMR (CD_3CN, $T = 263$ K): δ 18.3 (d, $^1J_{PtPA} = 1621$ Hz, $^2J_{PAPB} = 15.3$ Hz, P_A trans to Et), 13.2 (d, $^1J_{PtPB} = 4345$ Hz, $^2J_{PAPB} = 15.3$ Hz, P_B trans to MeCN).

***cis*-$[Pt(Et\text{-}d_5)(CH_3CN\text{-}d_3)(PEt_3)_2]^+$ (3a).** $^{31}P\{^1H\}$ NMR (CD_3CN, $T = 263$ K): δ 18.6 (d, $^1J_{PtPA} = 1609$ Hz, $^2J_{PAPB} = 17.8$ Hz, P_A trans to Et-d_5), 13.0 (d, $^1J_{PtPB} = 4352$ Hz, $^2J_{PAPB} = 17.8$ Hz, P_B trans to MeCN).

***cis*-$[Pt(Pr^n)(CH_3CN\text{-}d_3)(PEt_3)_2]^+$ (4a).** ^1H NMR (CD_3CN, $T = 263$ K): δ 1.41 (m, $^3J_{HH} = 7.7$ Hz, 12H, P_A-*CH*$_2$ + P_B-*CH*$_2$), 0.95−0.72 (m, 4H, Pt-(C*H*$_2$)$_2$-CH_3), 0.62 (m, $^3J_{HH} = 7.7$ Hz, 18H, P_A-*CH*$_3$ + P_B-*CH*$_3$), 0.45 (m, $^3J_{HH} = 7.7$ Hz, 3H, Pt-$(CH_2)_2$-*CH*$_3$). $^{31}P\{^1H\}$ NMR (CD_3CN, $T = 263$ K): δ 18.3 (d, $^1J_{PtPB} = 4312$ Hz, $^2J_{PAPB} = 15.3$ Hz, P_B trans to MeCN), 12.9 (d, $^1J_{PtPA} = 1657$ Hz, $^2J_{PAPB} = 15.3$ Hz, P_A trans to Pr^n).

***cis*-$[Pt(Bu^n)(CH_3CN\text{-}d_3)(PEt_3)_2]^+$ (5a).** ^1H NMR (CD_3CN, $T = 263$ K): δ 1.48 (m, $^3J_{HH} = 7.7$ Hz, 12H, P_A-*CH*$_2$ + P_B-*CH*$_2$), 1.08−0.85 (m, 6H, Pt-(*CH*$_2$)$_3$-CH_3), 0.69 (m, $^3J_{HH} = 7.7$ Hz, 18H, P_A-*CH*$_3$ + P_B-*CH*$_3$), 0.53 (m, 3H, Pt-$(CH_2)_3$-*CH*$_3$). $^{31}P\{^1H\}$ NMR (CD_3CN, $T = 263$ K): δ 18.3 (d, $^1J_{PtPA} = 1648$ Hz, $^2J_{PAPB} = 15.3$ Hz, P_A trans to Bu^n), 13.0 (d, $^1J_{PtPB} = 4331$ Hz, $^2J_{PAPB} = 15.3$ Hz, P_B trans to MeCN).

***cis*-$[Pt(CH_2\text{-}Si(CH_3)_3)(CH_3CN\text{-}d_3)(PEt_3)_2]^+$ (6a).** ^1H NMR (CD_3CN, $T = 298$ K): δ 1.67 (m, $^3J_{HH} = 7.7$ Hz, 12H, P_A-C*H*$_2$ + P_B-C*H*$_2$), 0.89 (m, $^3J_{HH} = 7.7$ Hz, 18H, P_A-C*H*$_3$ + P_B-C*H*$_3$), 0.25 (m, $^2J_{PtH} = 50.6$ Hz, $^3J_{HH} = 8.8$ Hz, 2H, Pt-C*H*$_2$), −0.15 (s, 9H, Si-*(CH*$_3$*)*$_3$). $^{31}P\{^1H\}$ NMR (CD_3CN, $T = 298$ K): δ 18.33 (d, $^1J_{PtPA} = 1890$ Hz, $^2J_{PAPB} = 17.8$ Hz, P_A trans to 2-MeC_6H_4), 10.28 (d, $^1J_{PtPB} = 4226$ Hz, $^2J_{PAPB} = 17.8$ Hz, P_B trans to MeCN).

***cis*-$[Pt(C_6H_5)(CH_3CN\text{-}d_3)(PEt_3)_2]^+$ (7a).** ^1H NMR (CD_3CN, $T = 298$ K): δ 7.07 (m, $^3J_{HH} = 6.6$ Hz, $^3J_{PtH} = 43.0$ Hz, 2H, *H*$_{2,6}$), 6.84 (dd, $^3J_{HH} = 7.7$ Hz, 2H, *H*$_{3,5}$), 6.72 (dd, $^3J_{HH} = 7.7$ Hz, 1H, *H*$_4$), 1.64 (m, $^3J_{HH} = 7.7$ Hz, 6H, P_A-C*H*$_2$), 1.40 (m, $^3J_{HH} = 7.7$ Hz, 6H, P_B-C*H*$_2$), 0.96 (m, $^3J_{HH} = 7.7$ Hz, 9H, P_A-C*H*$_3$), 0.79 (m, $^3J_{HH} = 7.7$ Hz, 9H, P_B-C*H*$_3$). $^{31}P\{^1H\}$ NMR (CD_3CN, $T = 298$ K): δ 15.0 (d, $^1J_{PtPA} = 1692$ Hz, $^2J_{PAPB} = 17.8$ Hz, P_A trans to C_6H_5), 7.4 (d, $^1J_{PtPB} = 4198$ Hz, $^2J_{PAPB} = 17.8$ Hz, P_B trans to MeCN).

***cis*-$[Pt(2\text{-}MeC_6H_4)(CH_3CN\text{-}d_3)(PEt_3)_2]^+$ (8a).** ^1H NMR (CD_3CN, $T = 298$ K): δ 7.1−6.9 (m, 1H, *H*$_6$), 6.78 (m, 1H, *H*$_3$), 6.71 (m, 2H, *H*$_{4,5}$), 2.25 (s, 3H, 2-C*H*$_3$), 1.72 (m, $^3J_{HH} = 8.8$ Hz, 6H, P_A-C*H*$_2$), 1.44 (m, $^3J_{HH} = 7.7$ Hz, 6H, P_B-C*H*$_2$), 0.98 (m, $^3J_{HH} = 7.7$ Hz, 9H, P_B-C*H*$_3$), 0.83 (m, $^3J_{HH} = 8.8$ Hz, 9H, P_A-C*H*$_3$). $^{31}P\{^1H\}$ NMR (CD_3CN, $T = 298$ K): δ 15.2 (d, $^1J_{PtPA} = 1653$ Hz, $^2J_{PAPB} = 17.8$ Hz, P_A trans to 2-MeC_6H_4), 5.7 (d, $^1J_{PtPB} = 4228$ Hz, $^2J_{PAPB} = 17.8$ Hz, P_B trans to MeCN).

***cis*-$[Pt(2,4,6\text{-}Me_3C_6H_2)(CH_3CN\text{-}d_3)(PEt_3)_2]^+$ (9a).** ^1H NMR (CD_3CN, $T = 298$ K): δ 6.48 (m, 2H, *H*$_{3,5}$), 2.24 (s, 6H, 2,2′-C*H*$_3$), 1.95 (s, 3H, *p*-C*H*$_3$), 1.73 (m, $^3J_{HH} = 7.7$ Hz, 6H, P_A-C*H*$_2$), 1.49 (m, $^3J_{HH} = 7.7$ Hz, 6H, P_B-C*H*$_2$), 0.98 (m, $^3J_{HH} = 7.7$ Hz, 9H, P_B-C*H*$_3$), 0.78 (m, $^3J_{HH} = 7.7$ Hz, 9H, P_A-C*H*$_3$). $^{31}P\{^1H\}$ NMR (CD_3CN, $T = 298$ K): δ 15.6 (d, $^1J_{PtPA} = 1644$ Hz, $^2J_{PAPB} = 17.8$ Hz, P_A trans to 2,4,6-$Me_3C_6H_2$), 2.8 (d, $^1J_{PtPB} = 4249$ Hz, $^2J_{PAPB} = 17.8$ Hz, P_B trans to MeCN).

Monoalkyl/aryl Solvent Complexes. (b) *trans*-$[Pt(R)(CH_3CN\text{-}d_3)(PEt_3)_2]^+$ (1b−9b). The spontaneous conversion of the cis solvent isomers (**1a**−**9a**) into their corresponding trans derivatives was obtained easily by setting aside at room temperature the solution resulting from the electrophilic attack on the corresponding dialkyl/aryl precursors. The process was complete in a few hours for R = Et, Et-d_5, Pr^n, and Bu^n (**2a**−**5a**), while many days were necessary for the remaining compounds (**1a** and **6a**−**9a**) containing alkyl/aryl groups with no β-hydrogens.

***trans*-$[Pt(Me)(CH_3CN\text{-}d_3)(PEt_3)_2]^+$ (1b).** ^1H NMR (CD_3CN, $T = 298$ K): δ 1.66 (m, $^3J_{HH} = 7.7$ Hz, 12H, P-*CH*$_2$-CH_3), 0.91 (m, $^3J_{HH} = 7.7$ Hz, 18H, P-CH_2-*CH*$_3$), 0.16 (m, $^2J_{PtH} = 81.4$ Hz, $^3J_{PH} = 14.3$ Hz, 3H, Pt-*CH*$_3$). $^{31}P\{^1H\}$ NMR (CD_3CN, $T = 298$ K): δ 22.8 ($^1J_{PtP} = 2687$ Hz).

***trans*-$[Pt(Et)(CH_3CN\text{-}d_3)(PEt_3)_2]^+$ (2b).** ^1H NMR (CD_3CN, $T = 298$ K): δ 1.76 (m, $^3J_{HH} = 7.7$ Hz, 2H, Pt-C*H*$_2$-CH_3), 1.54 (m, $^3J_{HH} = 7.7$ Hz, 12H, P-*CH*$_2$), 0.84 (m, $^3J_{HH} = 7.7$ Hz, 3H, Pt-CH_2-*CH*$_3$), 0.78 (m, $^3J_{HH} = 7.7$ Hz, 18H, P-*CH*$_3$). $^{31}P\{^1H\}$ NMR (CD_3CN, $T = 298$ K): δ 22.0 ($^1J_{PtP} = 2871$ Hz).

***trans*-$[Pt(Et\text{-}d_5)(CH_3CN\text{-}d_3)(PEt_3)_2]^+$ (3b).** $^{31}P\{^1H\}$ NMR (CD_3CN, $T = 298$ K): δ 22.5 ($^1J_{PtP} = 2848$ Hz).

***trans*-$[Pt(Pr^n)(CH_3CN\text{-}d_3)(PEt_3)_2]^+$ (4b).** ^1H NMR (CD_3CN, $T = 298$ K): δ 1.83−1.57 (m, $^3J_{HH} = 7.7$ Hz, 4H, Pt-(C*H*$_2$)$_2$-CH_3), 1.46 (m, $^3J_{HH} = 7.7$ Hz, 12H, P-*CH*$_2$), 0.71 (m, 18H, P-*CH*$_3$), 0.47 (m, 3H, Pt-$(CH_2)_2$-*CH*$_3$). $^{31}P\{^1H\}$ NMR (CD_3CN, $T = 298$ K): δ 21.9 ($^1J_{PtP} = 2857$ Hz).

***trans*-$[Pt(Bu^n)(CH_3CN\text{-}d_3)(PEt_3)_2]^+$ (5b).** ^1H NMR (CD_3CN, $T = 298$ K): δ 1.77−1.63 (m, 6H, Pt-(*CH*$_2$)$_3$-CH_3), 1.53 (m, $^3J_{HH} = 7.2$ Hz, 12H, P-*CH*$_2$), 0.77 (m, $^3J_{HH} = 7.2$ Hz, 18H, P-*CH*$_3$), 0.53 (m, 3H, Pt-$(CH_2)_3$-*CH*$_3$). $^{31}P\{^1H\}$ NMR (CD_3CN, $T = 298$ K): δ 21.7 ($^1J_{PtP} = 2861$ Hz).

***trans*-$[Pt(CH_2Si(CH_3)_3)(CH_3CN\text{-}d_3)(PEt_3)_2]^+$ (6b).** ^1H NMR (CD_3CN, $T = 298$ K): δ 1.72 (m, $^3J_{HH} = 7.7$ Hz, 12H, P-C*H*$_2$), 0.95 (m, $^3J_{HH} = 7.7$ Hz, 18H, P-C*H*$_3$), 0.16 (m, $^2J_{PtH} = 85.8$ Hz, $^3J_{PH} = 19.8$ Hz, 2H, Pt-*CH*$_2$), −0.21 (s, 9H, Si-*(CH*$_3$*)*$_3$). $^{31}P\{^1H\}$ NMR (CD_3CN, $T = 298$ K): δ 18.9 ($^1J_{PtP} = 2721$ Hz).

(54) (a) Van Geet, A. L. *Anal. Chem.* **1968**, *40*, 2227−2229. (b) Van Geet, A. L. *Anal. Chem.* **1970**, *42*, 679−680.
(55) Chatt, J.; Shaw, B. L. *J. Chem. Soc.* **1959**, 705−716.
(56) Chatt, J.; Shaw, B. L. *J. Chem. Soc.* **1959**, 4020−4033.
(57) Foley, P.; Di Cosimo, R.; Whitesides, G. M. *J. Am. Chem. Soc.* **1980**, *102*, 6713−6725.

***trans*-[Pt(C_6H_5)(CH_3CN-d_3)(PEt_3)$_2$]$^+$ (7b).** ^{1}H NMR (CD_3CN, T = 298 K): δ 6.97 (m, $^3J_{HH}$ = 6.6 Hz, $^3J_{PtH}$ = 60.5 Hz, 2H, $H_{2,6}$), 6.73 (dd, $^3J_{HH}$ = 7.7 Hz, 2H, $H_{3,5}$), 6.65 (dd, $^3J_{HH}$ = 7.7 Hz, 1H, H_4), 1.35 (m, $^3J_{HH}$ = 7.7 Hz, 12H, P-CH_2), 0.84 (m, $^3J_{HH}$ = 7.7 Hz, 18H, P-CH_3). ^{31}P{^{1}H} NMR (CD_3CN, T = 298 K): δ 20.1 ($^1J_{PtP}$ = 2679 Hz).

***trans*-[Pt(2-MeC_6H_4)(CH_3CN-d_3)(PEt_3)$_2$]$^+$ (8b).** ^{1}H NMR (CD_3CN, T = 298 K): δ 6.98 (m, $^3J_{HH}$ = 8.8 Hz, 1H, H_3), 6.77−6.56 (m, 3H, $H_{4,5,6}$), 2.20 (s, 3H, 2-CH_3), 1.40 (m, $^3J_{HH}$ = 8.8 Hz, 12H, P-CH_2), 0.86 (m, $^3J_{HH}$ = 8.8 Hz, 18H, P-CH_3). ^{31}P{^{1}H} NMR (CD_3CN, T = 298 K): δ 19.1 ($^1J_{PtP}$ = 2694 Hz).

***trans*-[Pt(2,4,6-$Me_3C_6H_2$)(CH_3CN-d_3)(PEt_3)$_2$]$^+$ (9b).** ^{1}H NMR (CD_3CN, T = 298 K): δ 6.43 (s, 2H, $H_{3,5}$), 2.20 (s, 3H, P-CH_3), 1.94 (s, 6H, 2,2′-CH_3), 1.40 (m, $^3J_{HH}$ = 7.7 Hz, 12H, P-CH_2), 0.85 (m, $^3J_{HH}$ = 7.7 Hz, 18H, P-CH_3). ^{31}P{^{1}H} NMR (CD_3CN, T = 298 K): δ 17.8 ($^1J_{PtP}$ = 2713 Hz).

Crystallography. Crystals of *cis*-[Pt(Bu^n)$_2$(PEt_3)$_2$], **5**, suitable for X-ray diffraction, were obtained by slow diffusion of hexane into a concentrated toluene solution and are air-stable. The unit cell constants, crystal symmetry determination, and data collection were carried out at 120(2) K, on a Bruker SMART CCD diffractometer. The space group was later confirmed by successful refinement. Selected crystallographic and other relevant data are listed in Tables 2 and 3 and in the Supporting Information. Data were corrected for Lorentz and polarization factors with the data reduction software SAINT[58] and empirically for absorption using the SADABS program.[59] The structure was solved by Patterson and Fourier methods and refined by full matrix least-squares analysis[60] (the function minimized being $[\sum w(F_o^2 - (1/k)F_c^2)^2]$ using anisotropic displacement parameters for all atoms except the hydrogen atoms; their contribution (in calculated position: C−H = 0.95 (Å); B (H) = $aB_{(Cbonded)}$ (Å^2), with a = 1.2 for CH_2 and a = 1.5 for the CH_3 groups) was included in the refinement using a riding model. No extinction correction was deemed necessary. The scattering factors used, corrected for the real and imaginary parts of the anomalous dispersion, were taken from the literature.[34] All calculations were carried out by using the WINGX,[61a] SHELX-97,[60] and ORTEP[61] programs.

Kinetic Measurements. The kinetic of isomerization of the *cis*-[Pt(R)(CH_3CN)(PEt_3)$_2$]$^+$ complexes (**1a**−**9a**) was followed spectrophotometrically by both traditional method, at constant temperature (CTK) for R = Et, Et-d_5, Pr^n, and Bu^n, and variable-temperature kinetics (VTK)[35,36,37] for R = Me, silyl, phenyl, *o*-tolyl, and mesityl.

(a) CTK Method. The reactions were started by adding with a syringe a prethermostated solution of complexes **2**−**5** in acetonitrile to a thermostated acetonitrile solution of $H^+BF_4^-$ in a silica cell, in the thermostated cell compartment of a spectrophotometer. A 1:1 acid/complex ratio was sufficient to produce a very fast cleavage of the first Pt−C bond. The kinetic of isomerization of **2a**−**5a** was followed by repetitive scanning of the spectrum at suitable times in the range of 350−200 nm. All the reactions obeyed a first-order rate law until well over 90% of the reaction and rate constant k_i (s^{-1}) was obtained from a nonlinear least-squares fit of the experimental data to $D_t = D\infty + (D_0 - D\infty)\exp(-k_i t)$ with D_0, $D\infty$, and k_i as the parameters to be optimized (D_0 = absorbance after mixing of reagents and $D\infty$ = absorbance at completion of reaction). Activation parameters were derived from a linear least-squares analysis of $\ln(k_i/T)$ versus T^{-1} according to the Eyring equation

$$k = (kT/h)\exp(-\Delta H^{\ddagger}/RT)\exp(\Delta S^{\ddagger}/R) \qquad (2)$$

and are listed in Table 4.

(b) VTK Method. Kinetic runs were carried out using a JASCO V-560 spectrophotometer, connected to a Pentium II 800 MHz computer. The reaction cell was equipped with a stirrer to ensure chemical and thermal homogeneity, and the cell compartment was connected to a HAAKE C 25 thermostating bath that allows a controlled change of the temperature with time with an accuracy of ±0.05 °C. The temperature was checked by a platinum resistor inserted into the spectrophotometric cell and connected to the computer (readout resolution 0.01 °C). The reactions were started as described previously for the CTK method. The reactions were followed at a fixed wavelength, and the absorbance−temperature−time data were automatically acquired by using a Visual Basic program. The starting temperature (T_0) was made sufficiently low to slow down the initial rate of reaction and to make negligible the dead-time before reaching the linear part of the temperature program. The acquisition speed was adjusted to have a good density of points and a good fit to the mathematical model. The processing of the stored data was performed by use of the MicroMath SCIENTIST program[62] with a Powell modified Marquadt algorithm[63] for the fitting and the Eulero method for solving the differential equation

$$-\frac{d(D_t - D\infty)}{dt} = \frac{k(T_0 + \alpha_t)}{h}\exp\left[\frac{\Delta S^{\ddagger}}{R}\right]\exp\left[-\frac{\Delta H^{\ddagger}}{R(T_0 + \alpha t)}\right](D_t - D\infty) \qquad (3)$$

where α is the temperature gradient, and $D\infty$, $\Delta H^{\ddagger}$, and $\Delta S^{\ddagger}$ are the parameters to be optimized. The k_i versus T profile of Figure SI1B in the Supporting Information has been obtained simply by dividing the time derivative of the absorbance data in Figure 3 to the normalized value of the absorbance ($D_t - D\infty$).

Computational Details. Geometry optimizations as well as frequency calculations for all the model complexes considered here were performed at the density functional level of theory, employing the Becke's three-parameter hybrid functional[64] combined with the Lee−Yang−Parr (LYP)[65] correlation functional, denoted as B3LYP within the Gaussian 03/DFT package.[66] The LANL2DZ effective core potential[67] was used for the metal center. In LANL2DZ, the valence shell is explicitly represented using double-ζ and includes both n = 5(s,p,d) and n = 6(s) orbitals. The standard 6-31+G** basis set[68] was employed for the rest of the atoms.

No symmetry restrictions were imposed during the geometry optimizations, whereas for each optimized stationary point, vibrational analysis was performed to determine its character (minimum or saddle point) and to evaluate the zero-point vibrational energy (ZPVE) corrections, which are included in all relative energies. For all the reported transition states, it was carefully checked that the vibrational mode associated with the imaginary frequency corresponds to the correct movement of involved atoms. All the minima connected by a given transition state were confirmed by intrinsic reaction coordinate (IRC)[69] driving calculations (in mass-weighted coordinates) as implemented in the Gaussian 03 program.

Acknowledgment. We are grateful to the Ministero dell' Università e della Ricerca Scientifica e Tecnologica (MIUR),

(58) *Bruker AXS, SAINT, Integration Software*; Bruker Analytical X-ray Systems: Madison, WI, 1995.
(59) Sheldrick, G. M. *SADABS, Program for Absorption Correction*; University of Göttingen: Göttingen, Germany, 1996.
(60) Sheldrick, G. M. *SHELX-97, Structure Solution and Refinement Package*; University of Göttingen: Göttingen, Germany, 1997.
(61) (a) Farrugia, L. J. *J. Appl. Crystallogr.* **1999**, *32*, 837−838. (b) Farrugia, L. J. *J. Appl. Crystallogr.* **1997**, *30*, 565.
(62) MicroMath Scientific Software; Micromath: Salt Lake City, UT.
(63) Press, W. H.; Flannery, B. P.; Teukolsky, S. A.; Vetterling, W. T. *Numerical Recipes*; Cambridge University Press: Cambridge, 1986.
(64) Becke, A. D. *J. Chem. Phys.* **1993**, *98*, 5648−5652.
(65) Stephens, P. J.; Devlin, F. J.; Chabalowski, C. F.; Frisch, M. J. *J. Phys. Chem.* **1994**, *98*, 11623−11627.
(66) Frisch, M. J. et al. *Gaussian 03*, revision A.1; Gaussian, Inc.: Pittsburgh, PA, 2003.
(67) (a) Hay, P. J.; Wadt, W. R. *J. Chem. Phys.* **1985**, *82*, 270−283. (b) Wadt, W. R.; Hay, P. J. *J. Chem. Phys.* **1985**, *82*, 284−298. (c) Hay, P. J.; Wadt, W. R. *J. Chem. Phys*. **1985**, *82*, 299.
(68) (a) Krishnan, R.; Binkley, J. S.; Seeger, R.; Pople, J. A. *J. Chem. Phys*. **1980**, *72*, 650−654. (b) Blaudeau, J. P.; McGrath, M. P.; Curtiss, L. A.; Radom, L. *J. Chem. Phys*. **1997**, *107*, 5016−5021.
(69) (a) Gonzalez, C.; Schlegel, H. B. *J. Chem. Phys*. **1989**, *90*, 2154−2161. (b) Gonzalez, C.; Schlegel, H. B. *J. Phys. Chem.* **1990**, *94*, 5523−5527.

PRIN 2004, and to the University of Messina, PRA 2003, for funding this work.

Supporting Information Available: Figure of spectral changes associated with isomerization of **6a** at constant temperature and k_i vs T profile for the same reaction obtained from the analysis of the VTK kinetic run in Figure 3. Figure of an example of ^{31}P NMR spectra of *cis*- and *trans*-$[Pt(Et)(PEt_3)_2(CD_3CN)]^+$ compounds in acetonitrile-d_3. Tables of a full listing and assignment of ^{1}H and ^{31}P NMR data for compounds **1**−**9**, the temperature dependence of primary kinetic data for **1a**−**9a**, and Cartesian coordinates of the B3LYP optimized T-shaped *cis*- and *trans*-$[Pt(R)(PMe_3)_2]^+$ (R = Me, Et, Bu^n) complexes. Extended tables of crystallographic data, coordinates, ADPs, bond distances, bond angles, and torsion angles. Complete list of authors for ref 66. This material is available free of charge via the Internet at http://pubs.acs.org.

JA0702162